Beyond the Dipole
The resilience of the RVM in magnetars with extended emission regions

Finanziato dall'Unione europea
NextGenerationEU

Ministero dell'Università e della Ricerca

Italiadomani
PIANO NAZIONALE DI RIPRESA E RESILIENZA

Dipartimento di Fisica e Astronomia
UNIVERSITÀ DEGLI STUDI DI PADOVA

Dipartimento di Fisica e Astronomia
UNIVERSITÀ DEGLI STUDI DI PADOVA

ISSI Team 25-657
Polarimetric Insight into Extreme Magnetism

A bit of history

- PA variation with photon energy initially ascribed to Faraday rotation (Smith, 1968)

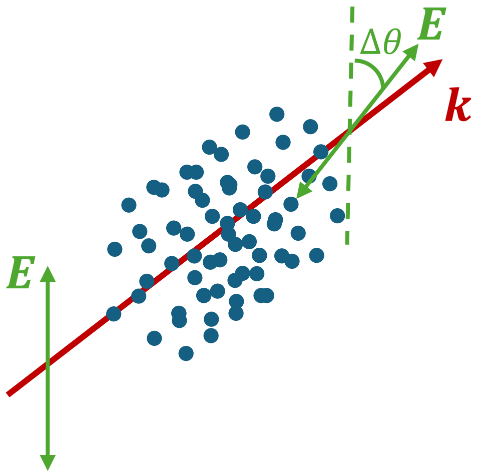

- Linearly polarized radiation passing through a plasma in the presence of B-field undergoes a rotation of the polarization plane

$$\Delta\theta \sim \lambda^2 \int n_e \boldsymbol{B} \cdot d\ell$$

A bit of history

- PA variation with photon energy initially ascribed to Faraday rotation (Smith, 1968)

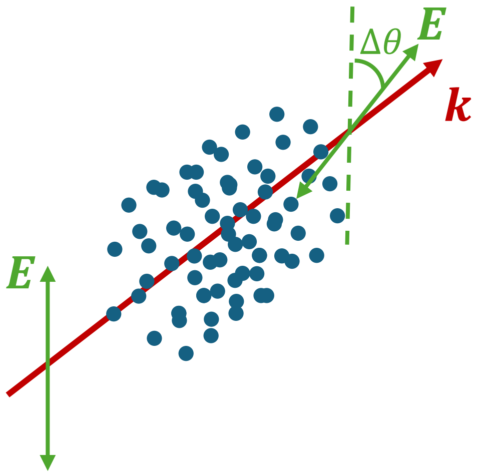

- Linearly polarized radiation passing through a plasma in the presence of B-field undergoes a rotation of the polarization plane

$$\Delta\theta \sim \lambda^2 \int n_e \boldsymbol{B} \cdot d\ell$$

Proportionality to λ^2

A bit of history

- PA variation with photon energy initially ascribed to Faraday rotation (Smith, 1968)

- This predicted behavior is very well observed in the radio band (e.g. Radhakrishnan & Cooke, 1969)

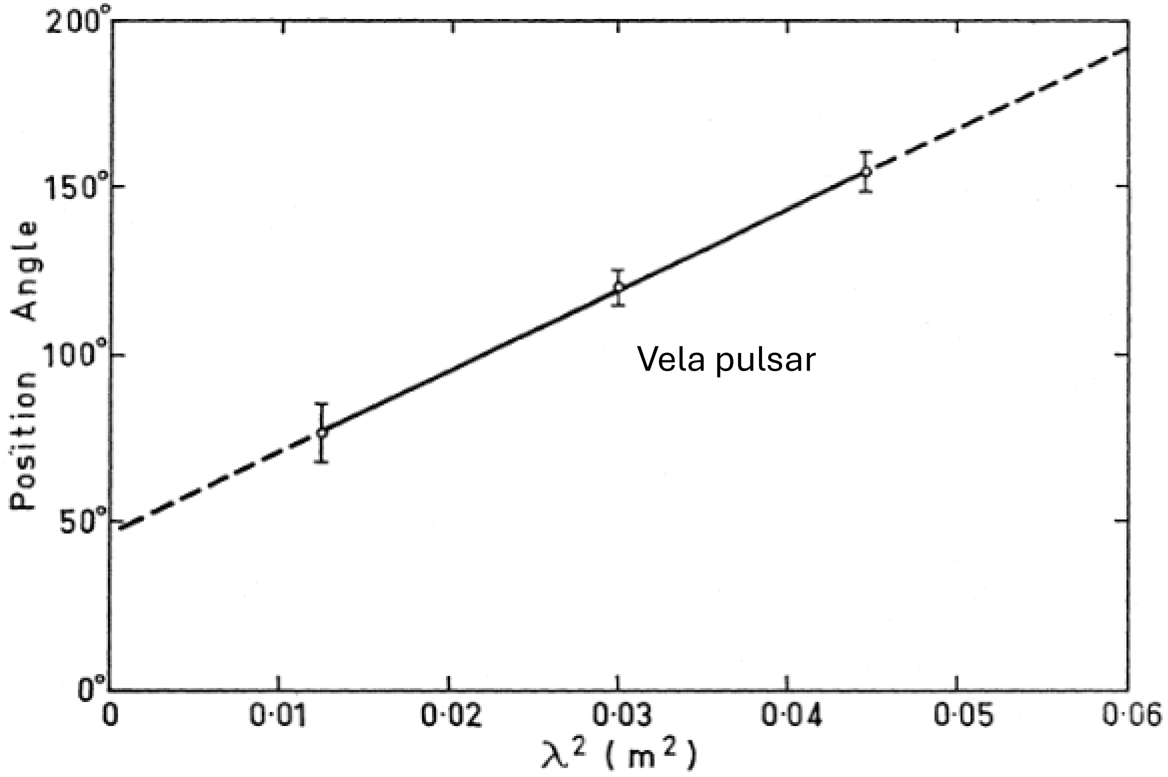

FIG. 1. The position angle of the peak of the pulse at 2700, 1720, and 1420 MHz plotted against the square of the wavelength. The slope of the line corresponds to a rotation measure of $+42\pm4$ rad m^{-2}.

Radhakrishnan & Cooke (1969)

A bit of history

- The situation changed when the temporal evolution of PA was taken into account

Change of PA with time
$\approx 90°$ in 4 ms
($P_{\rm NS} \approx 89$ ms)

Difference of PA measured in two bands
(constant during the pulse)

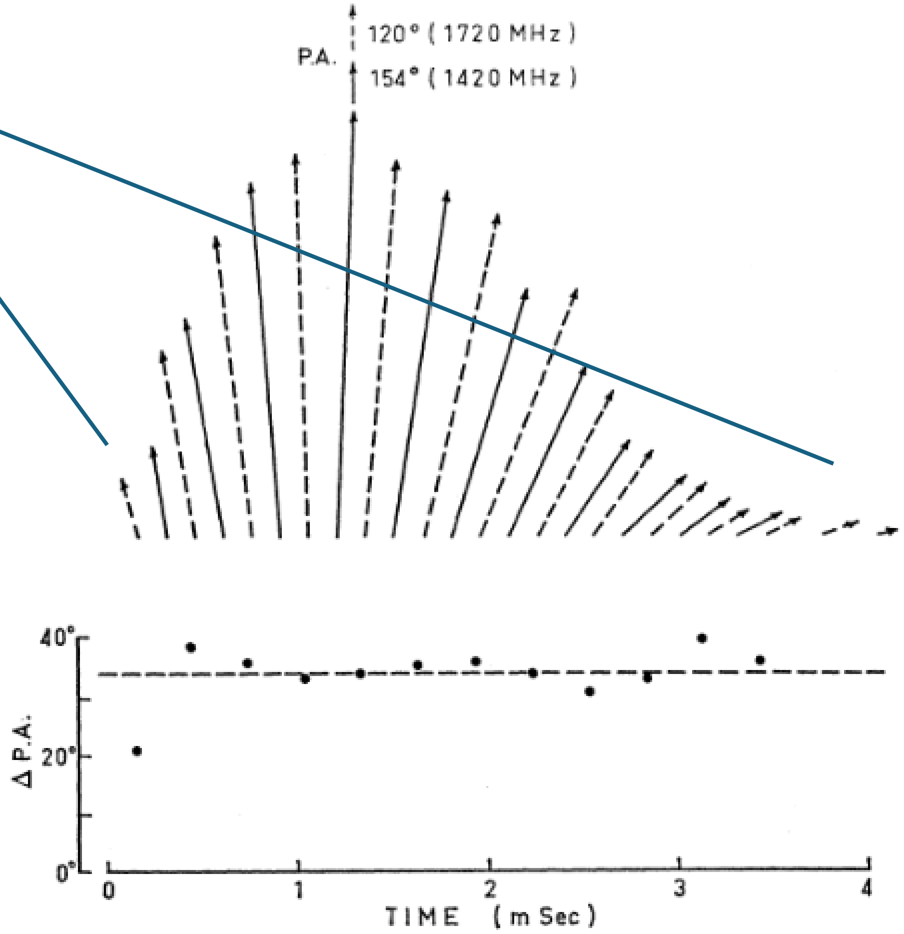

Radhakrishnan & Cooke (1969)

A bit of history

- The situation changed when the temporal evolution of PA was taken into account

- Spin velocity $\rightarrow\ \approx 4\ \mathrm{deg/ms}$
- PA-change velocity $\rightarrow\ \approx 23\ \mathrm{deg/ms}$

Polar effect

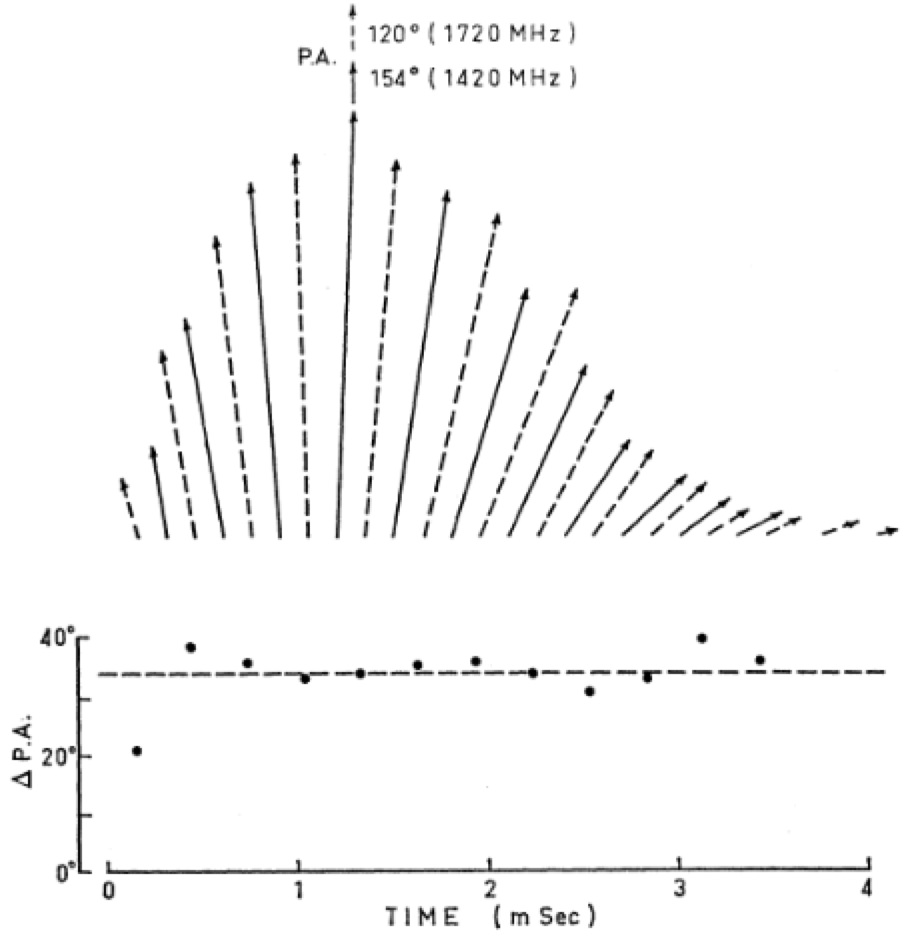

Radhakrishnan & Cooke (1969)

A bit of history

- The situation changed when the temporal evolution of PA was taken into account

- Spin velocity $\rightarrow$ $\approx 4\ \text{deg/ms}$
- PA-change velocity $\rightarrow$ $\approx 23\ \text{deg/ms}$

Polar effect

- Polarization is determined by the B-field

Magnetic pole

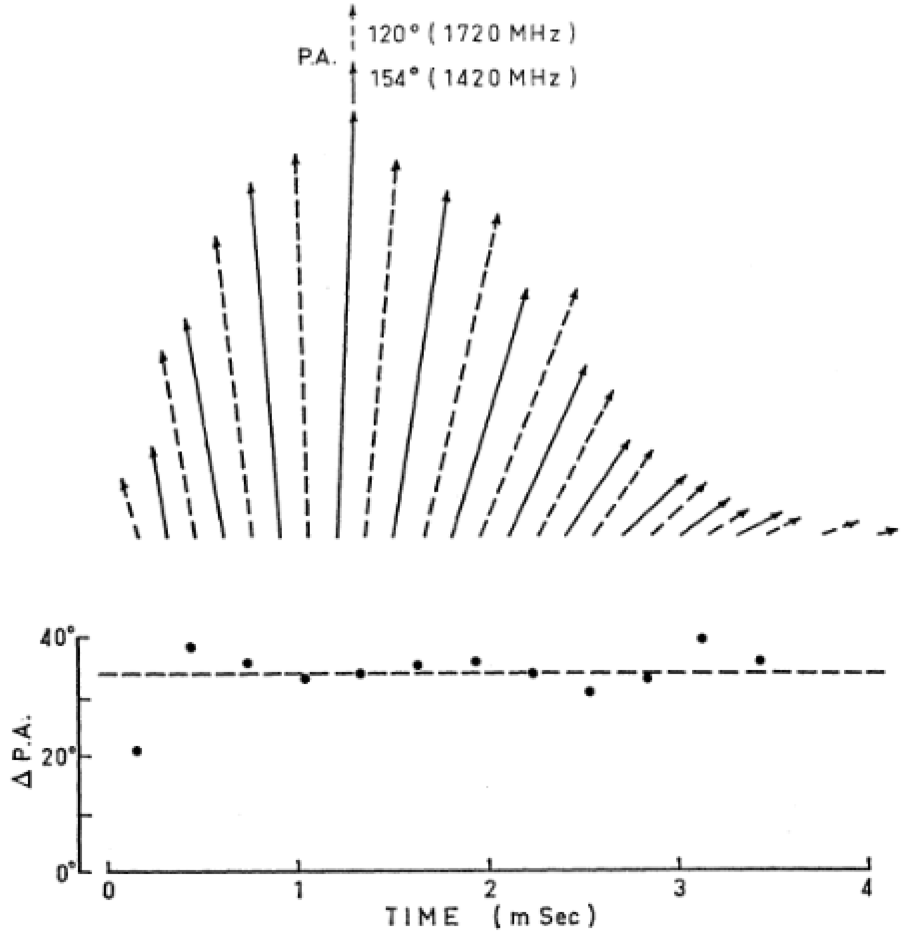

Radhakrishnan & Cooke (1969)

A bit of history

- The situation changed when the temporal evolution of PA was taken into account

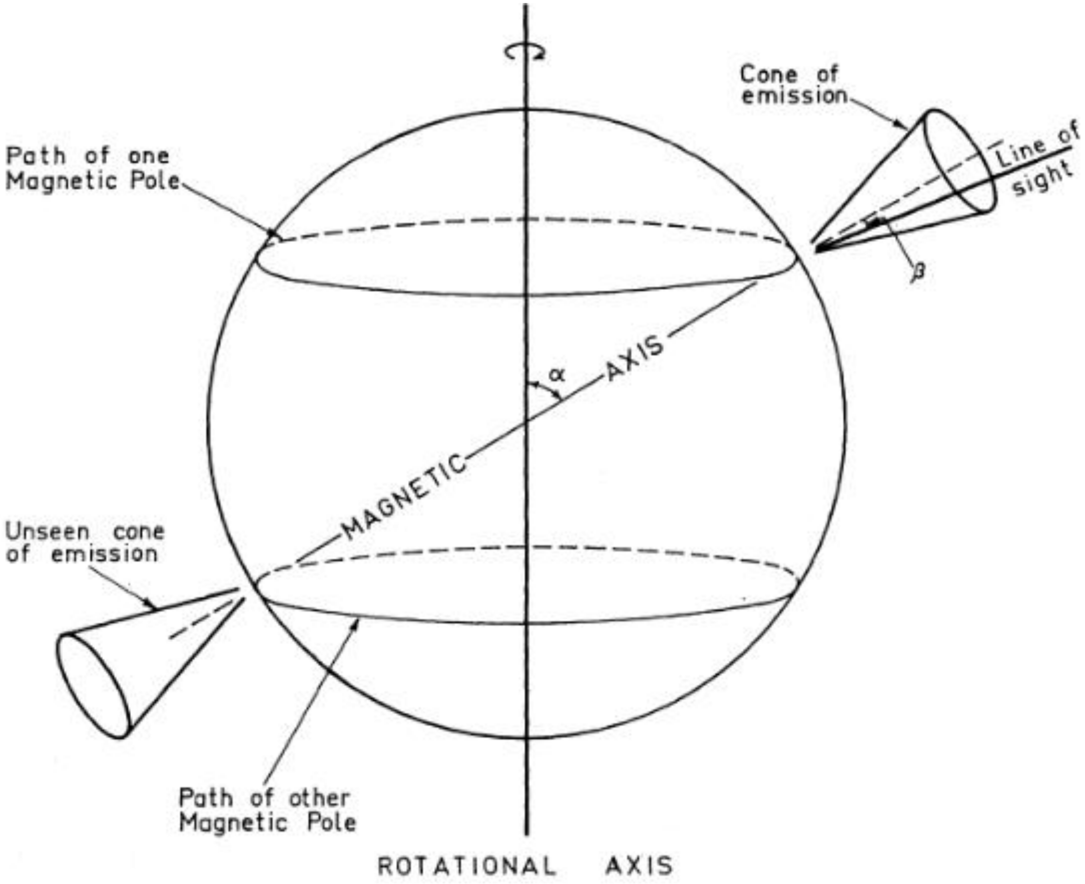

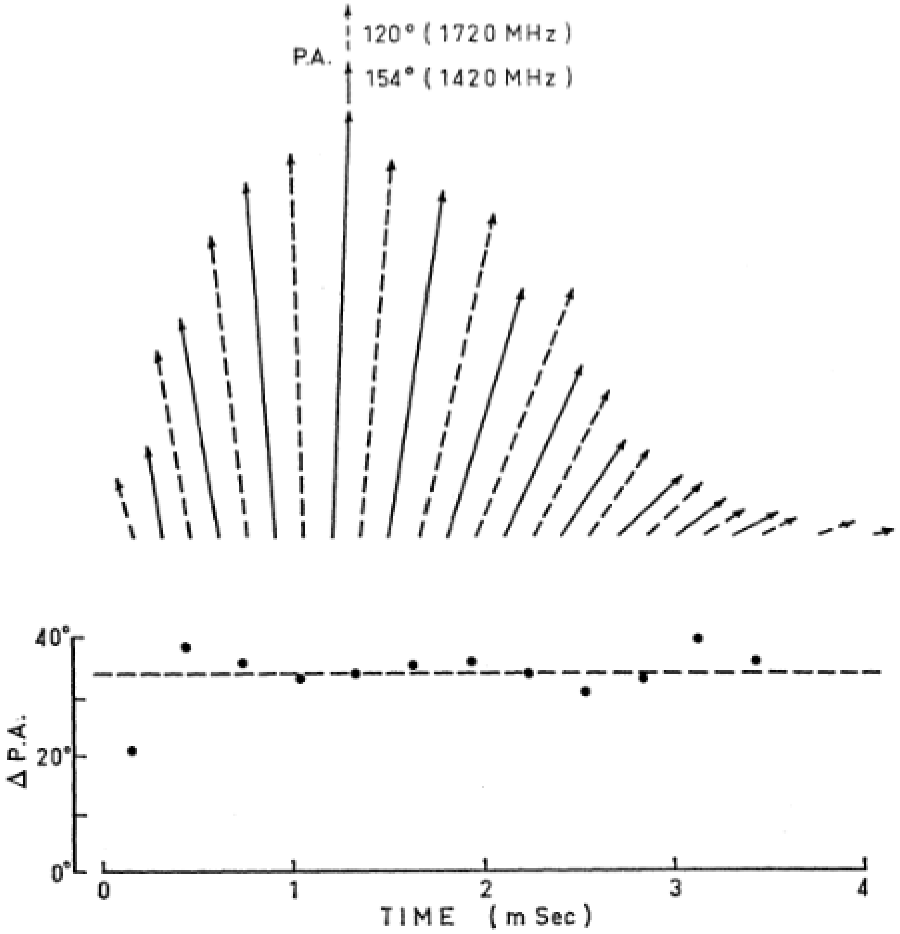

Radhakrishnan & Cooke (1969)

The Rotating Vector Model

- Komesaroff (1970) first formalized this geometrical effect as the rotation of the magnetic-dipole axis projection in the plane of the sky

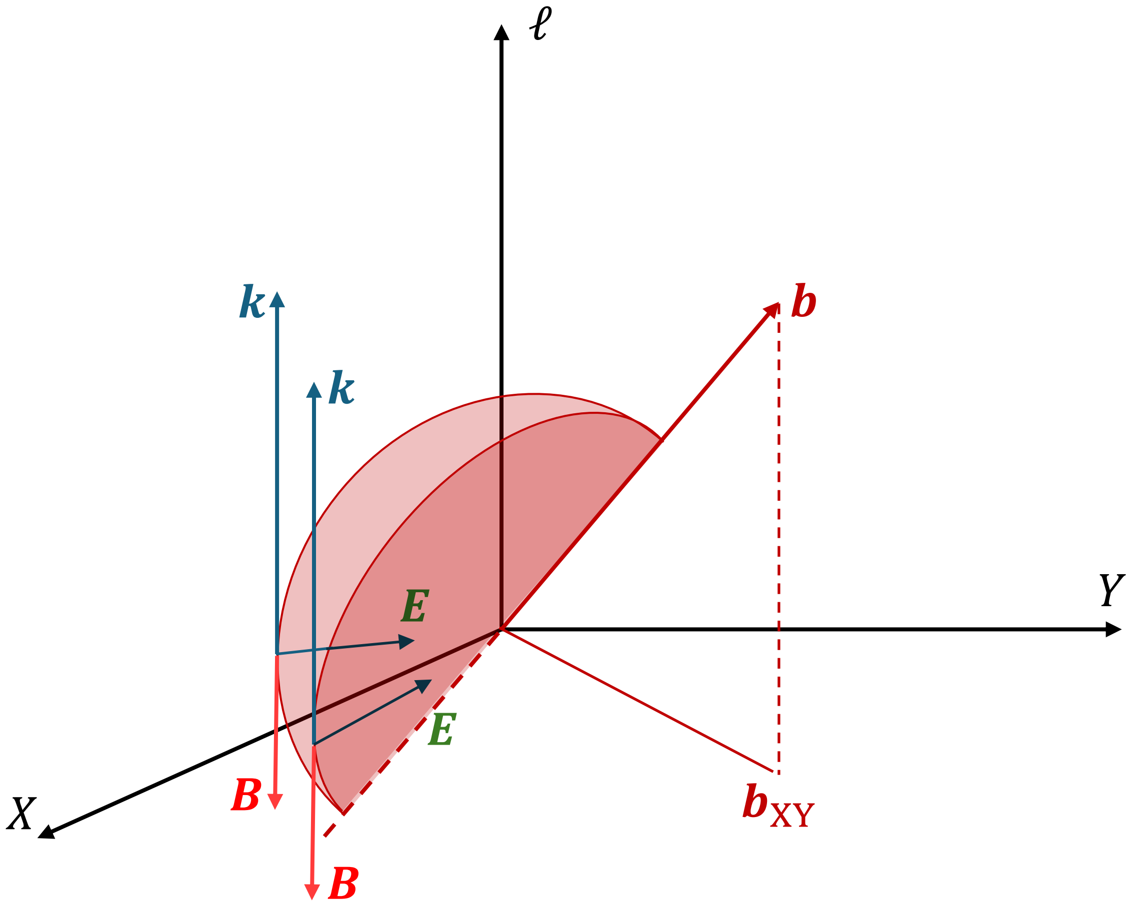

Curvature emission ($\boldsymbol{k} \parallel \boldsymbol{B}$, tangent):

- polarization vectors $\boldsymbol{E}$ lie in the plane of the field line, parallel to the particle $\boldsymbol{a}$;

Dipolar magnetic field:

- the field lines are contained in a single meridional plane;
- all the planes share in common the magnetic axis direction

$\Rightarrow$ **$\boldsymbol{E}$ position angle $= \boldsymbol{b}_{XY}$ position angle**

The Rotating Vector Model

- Komesaroff (1970) first formalized this geometrical effect as the rotation of the magnetic-dipole axis projection in the plane of the sky

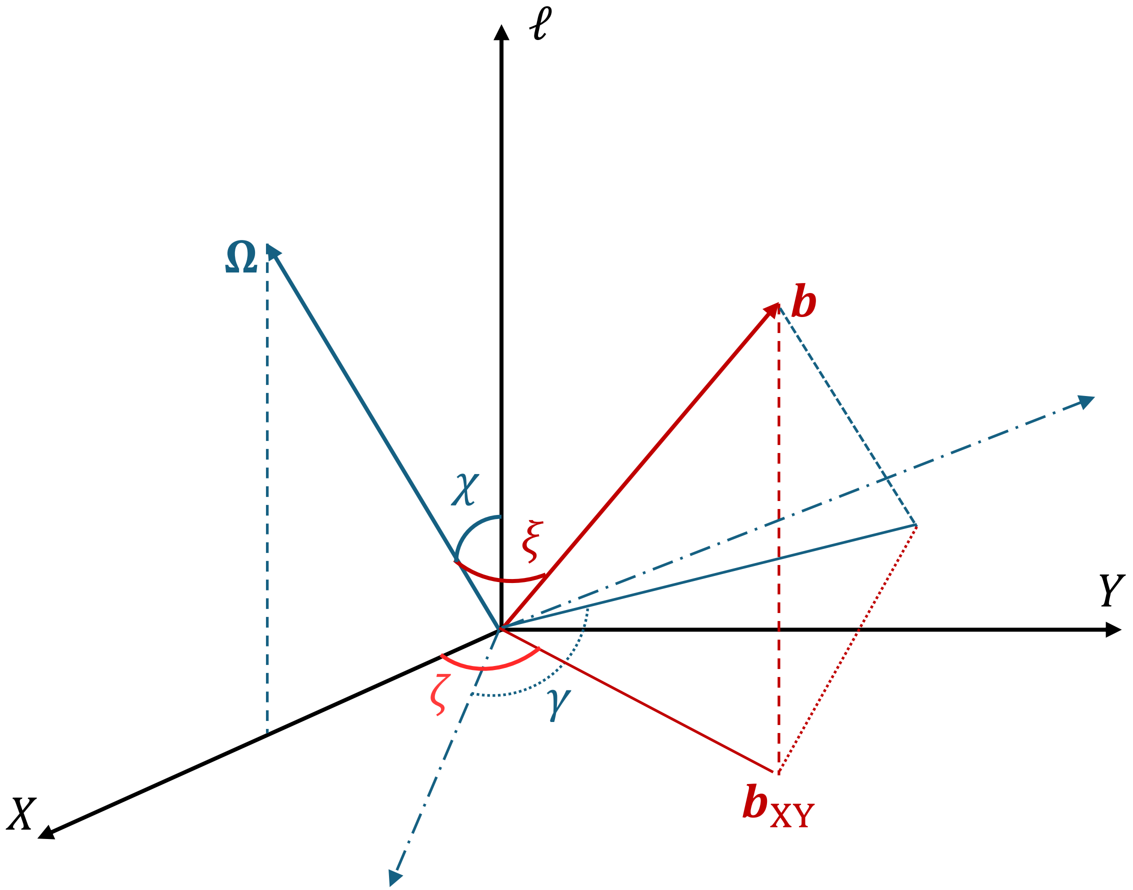

ℓ: LOS – $\boldsymbol{\Omega}$: spin axis – $\boldsymbol{b}$: magnetic axis

χ: ℓ-$\boldsymbol{\Omega}$ inclination – ξ: $\boldsymbol{b}$-$\boldsymbol{\Omega}$ inclination

γ: rotational phase

ζ: $\boldsymbol{b}$ position angle wrt the projection of $\boldsymbol{\Omega}$ onto the plane of the sky

The Rotating Vector Model

- Komesaroff (1970) first formalized this geometrical effect as the rotation of the magnetic-dipole axis projection in the plane of the sky

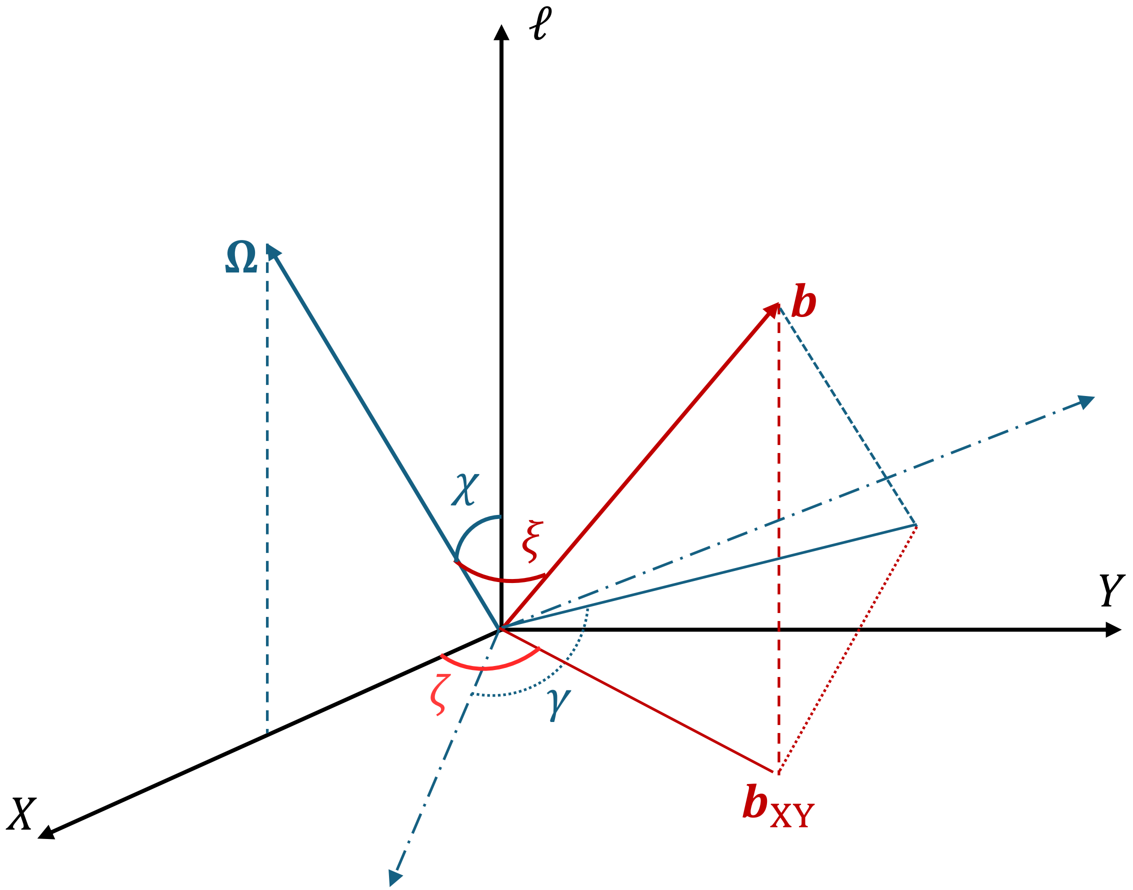

In the LOS frame $XY\ell$

$$\boldsymbol{b} = \begin{pmatrix} \sin\chi\cos\xi - \cos\chi\sin\xi\cos\gamma \\ \sin\xi\sin\gamma \\ \cos\chi\cos\xi + \sin\chi\sin\xi\cos\gamma \end{pmatrix} \qquad \ell = \begin{pmatrix} 0 \\ 0 \\ 1 \end{pmatrix}$$

The Rotating Vector Model

- Komesaroff (1970) first formalized this geometrical effect as the rotation of the magnetic-dipole axis projection in the plane of the sky

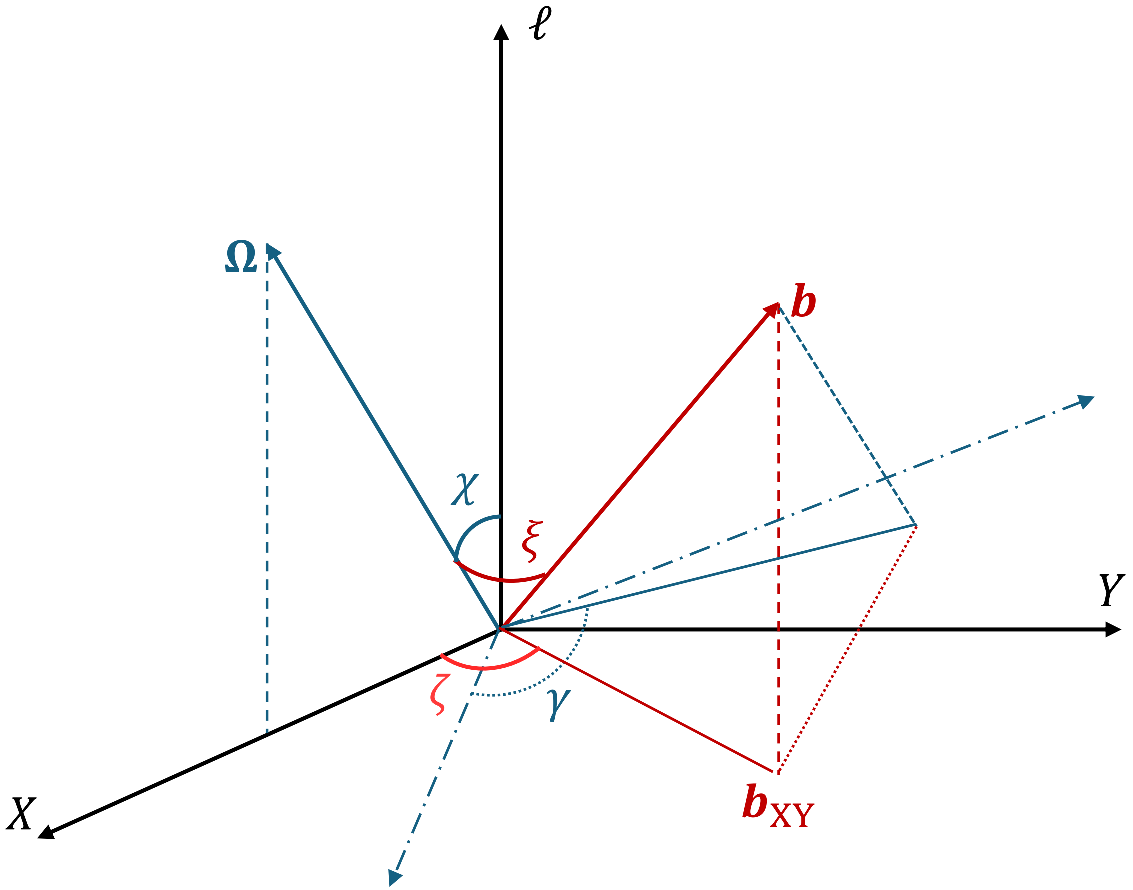

In the LOS frame $XY\ell$

$$\boldsymbol{b} = \begin{pmatrix} \sin\chi\cos\xi - \cos\chi\sin\xi\cos\gamma \\ \sin\xi\sin\gamma \\ \cos\chi\cos\xi + \sin\chi\sin\xi\cos\gamma \end{pmatrix} \qquad \ell = \begin{pmatrix} 0 \\ 0 \\ 1 \end{pmatrix}$$

$$\boldsymbol{b}_{XY} = \begin{pmatrix} \sin\chi\cos\xi - \cos\chi\sin\xi\cos\gamma \\ \sin\xi\sin\gamma \\ 0 \end{pmatrix}$$

$$\cos\zeta = \sin\chi\cos\xi - \cos\chi\sin\xi\cos\gamma \qquad \sin\zeta = \sin\xi\sin\gamma$$

$$\Rightarrow \quad \boxed{\tan\zeta = \frac{\sin\xi\sin\gamma}{\sin\chi\cos\xi - \cos\chi\sin\xi\cos\gamma}}$$

The Rotating Vector Model

- Komesaroff (1970) first formalized this geometrical effect as the rotation of the magnetic-dipole axis projection in the plane of the sky

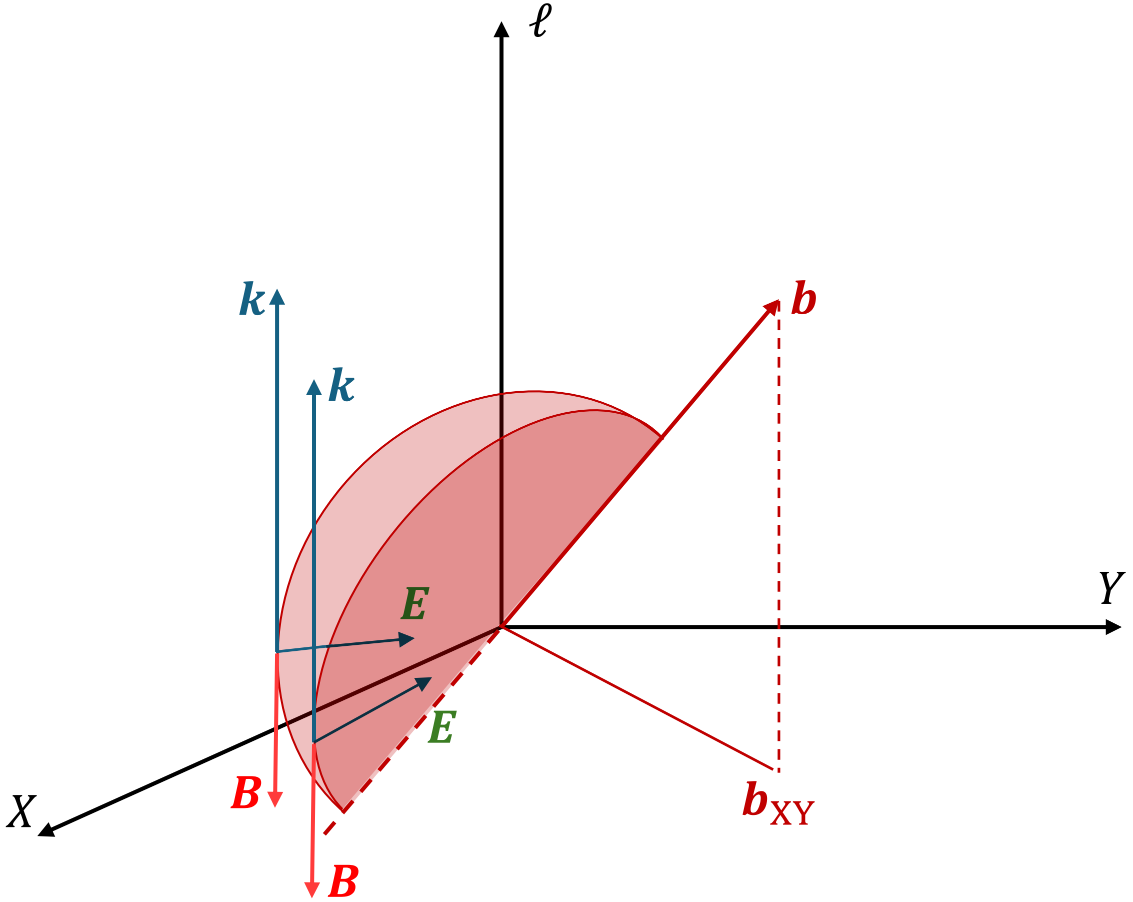

Statistical behavior

- not comparing the single E-vector but their (vectorial sum)

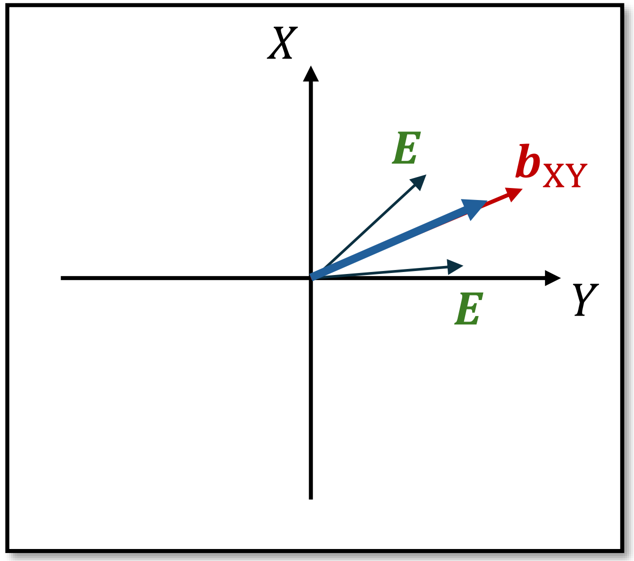

The Rotating Vector Model

- Komesaroff (1970) first formalized this geometrical effect as the rotation of the magnetic-dipole axis projection in the plane of the sky

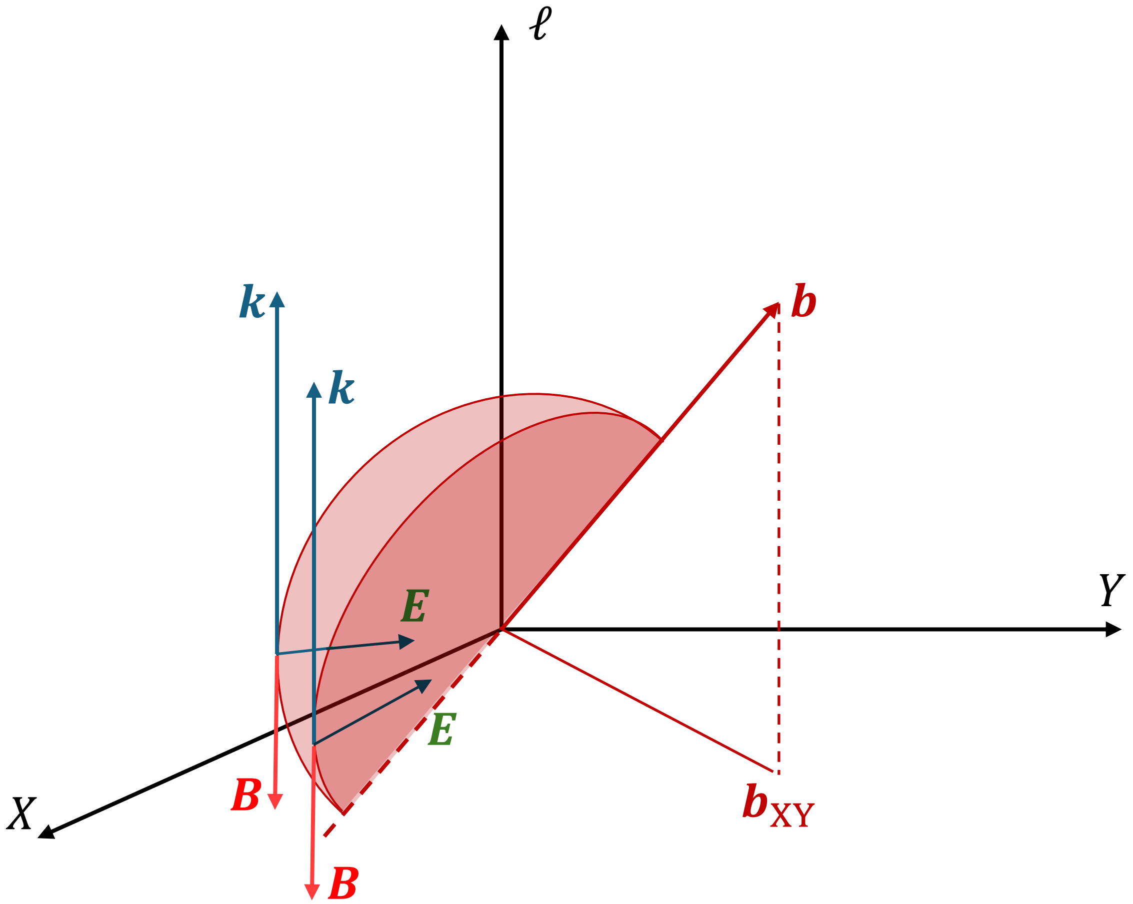

Statistical behavior

- not comparing the single E-vector but their (vectorial sum)

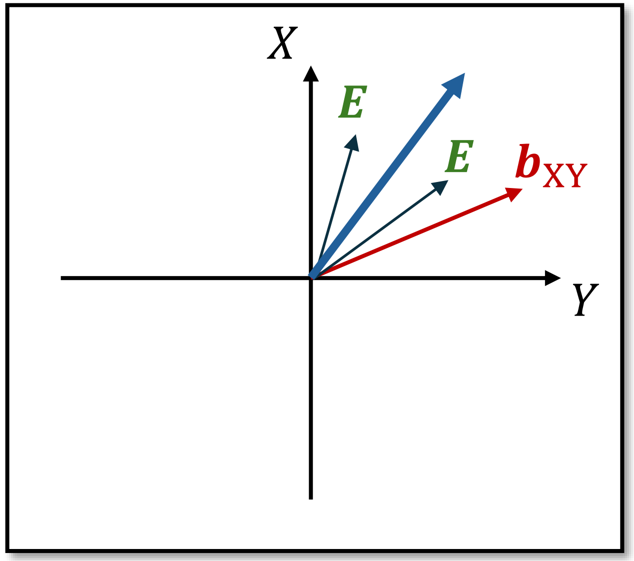

The Rotating Vector Model

- Komesaroff (1970) first formalized this geometrical effect as the rotation of the magnetic-dipole axis projection in the plane of the sky

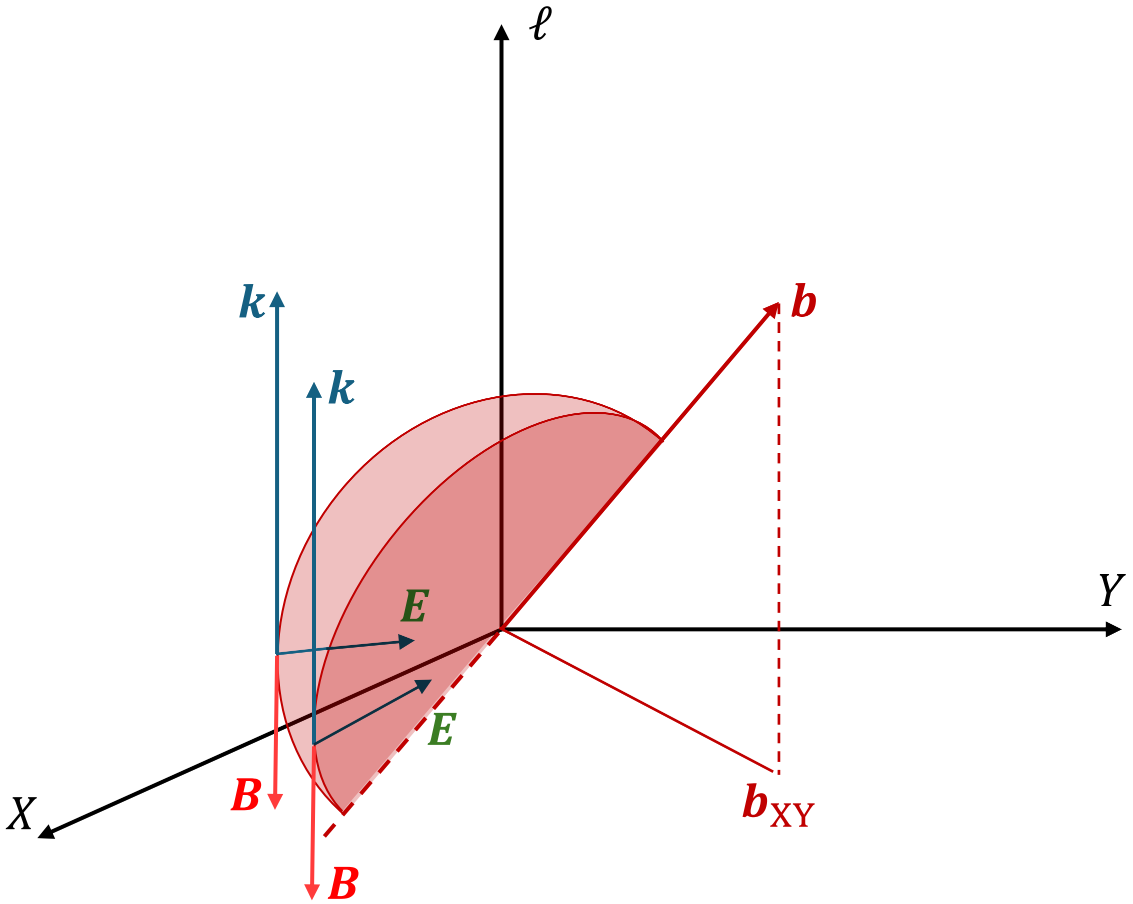

If the emission region is azimuthally symmetric?

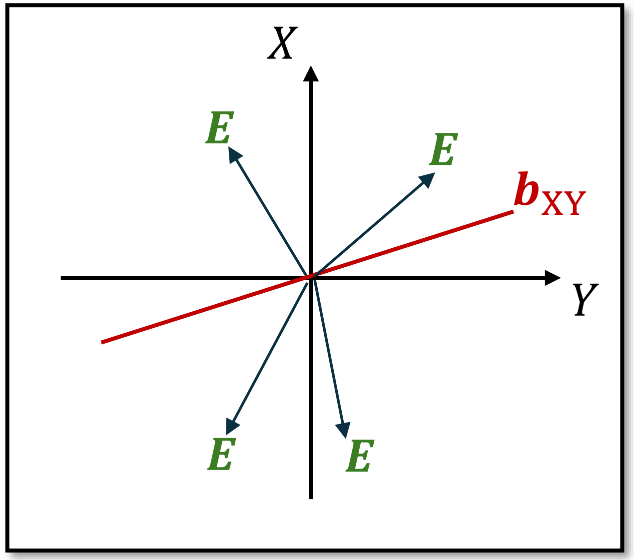

The Rotating Vector Model

- Komesaroff (1970) first formalized this geometrical effect as the rotation of the magnetic-dipole axis projection in the plane of the sky

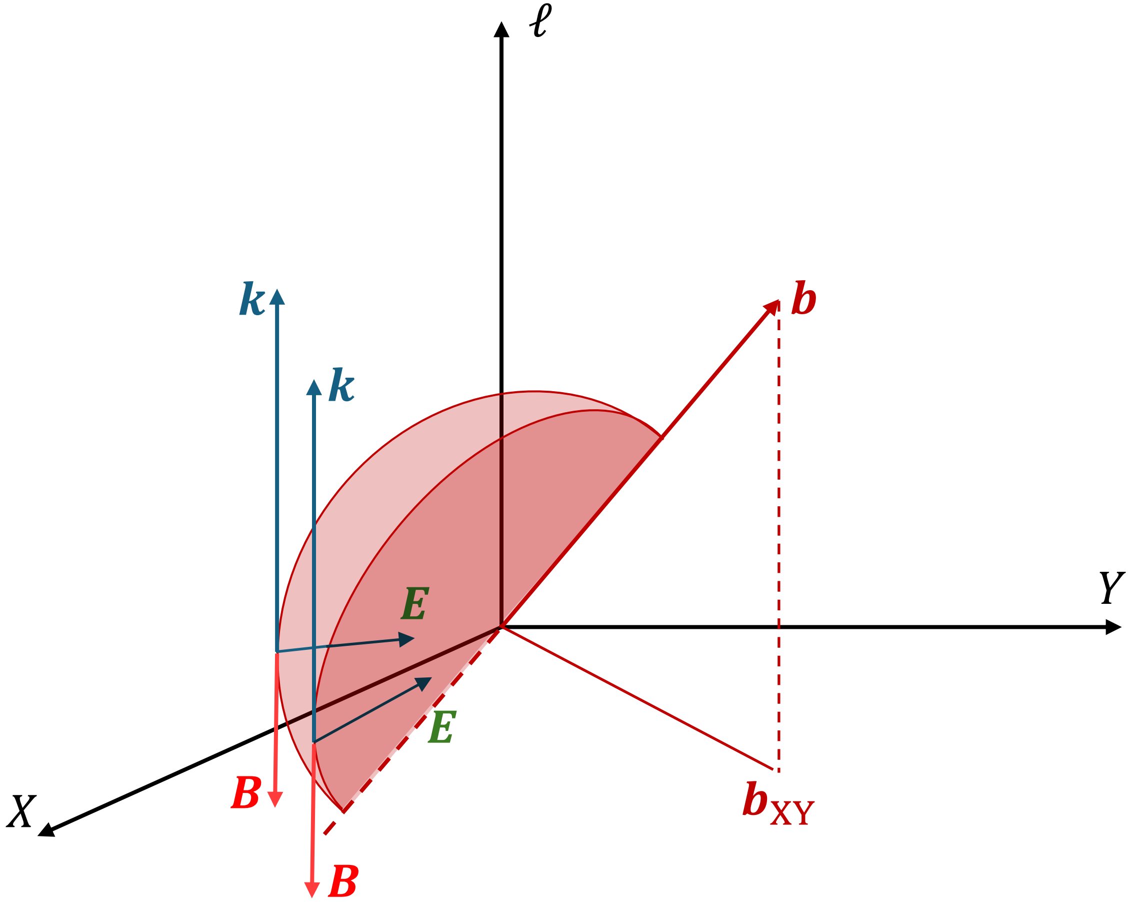

If the emission region is azimuthally symmetric?

Weighting with intensity (scaling with colatitude θ)

$$I(\theta) \sim \frac{3\sin^2\theta\left(1+\cos^2\theta\right)^2}{(1+3\cos^2\theta)^3};$$

T

- Ko … on of the … but … th

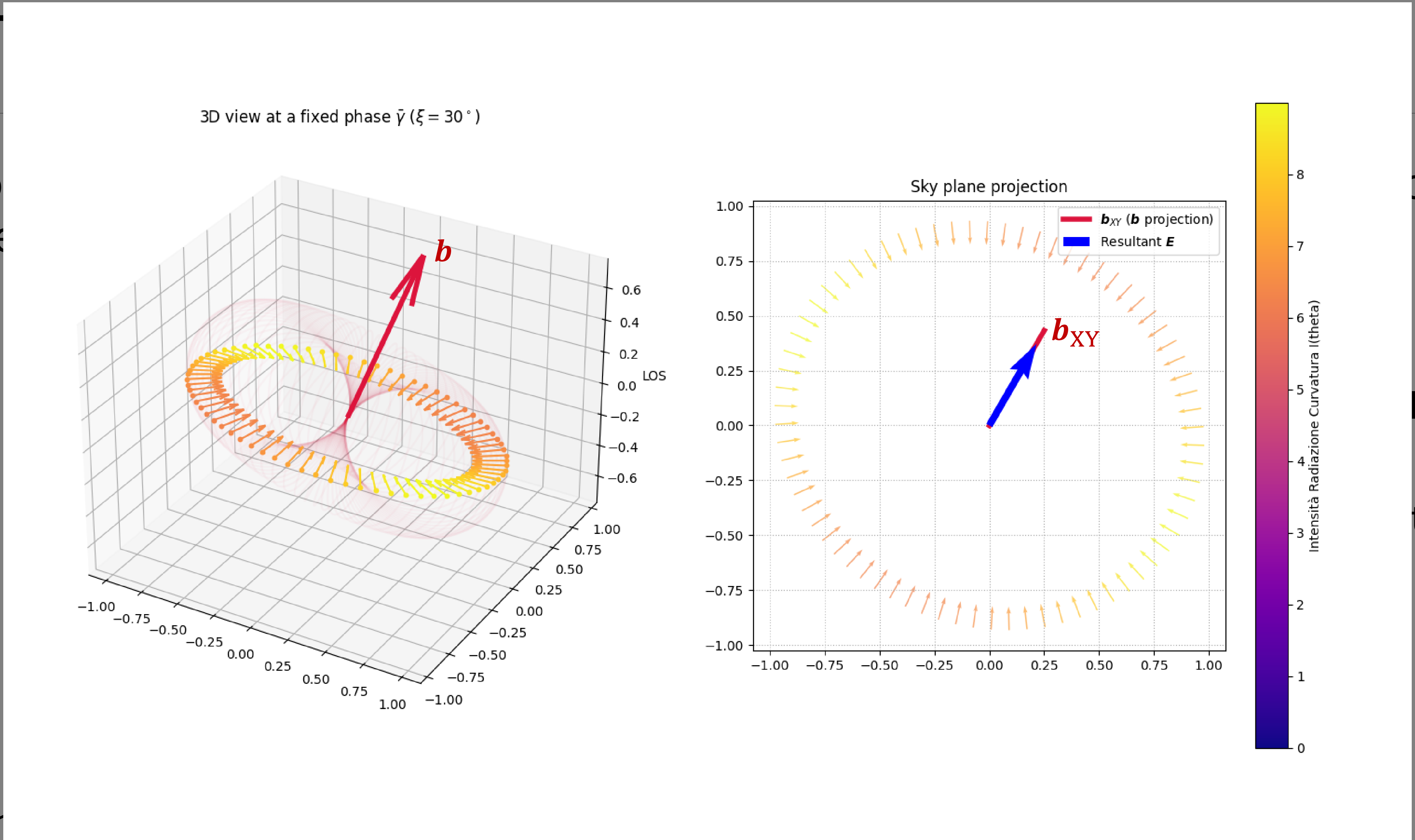

X

B

The Rotating Vector Model

- Komesaroff (1970) first formalized this geometrical effect as the rotation of the magnetic-dipole axis projection in the plane of the sky

- «Global» polarization vector projected in the plane of the sky coincides with the projection of $\boldsymbol{b}$

- Requirements:
  - Dipolar field (axissymmetric, magnetic field lines lie in the same «meridional» plane)
  - Curvature radiation (coming from «tangential points», polarization along $\boldsymbol{a}$, specific intensity law with θ)

- RVM reflects a **statistical** behavior

The Rotating Vector Model – CORRECTED

- The simple geometric expression used by Komesaroff (1970) and Manchester & Taylor (1977) needs corrections due to
  - star rotation at large velocities;
  - GR corrections (ray-bending)

- Poutanen (2020, see also Viironen & Poutanen, 2004) provided a corrected model for both effects

$$\tan\chi = \frac{\sin\theta\sin\phi + \beta A}{-\sin i\cos\theta + \cos i\sin\theta\cos\phi - \beta\sin\phi\, C}, \quad (58)$$

where

$$A = \frac{\sin\psi}{\sin\alpha} B + \frac{\cos\alpha - \cos\psi}{\sin\alpha\sin\psi}(\cos\phi - B\cos\psi),$$

$$B = \sin i\sin\theta + \cos i\cos\theta\cos\phi, \quad (59)$$

$$C = \frac{\sin\psi}{\sin\alpha}\cos\theta + \frac{\cos\alpha - \cos\psi}{\sin\alpha\sin\psi}(\cos i - \cos\theta\cos\psi).$$

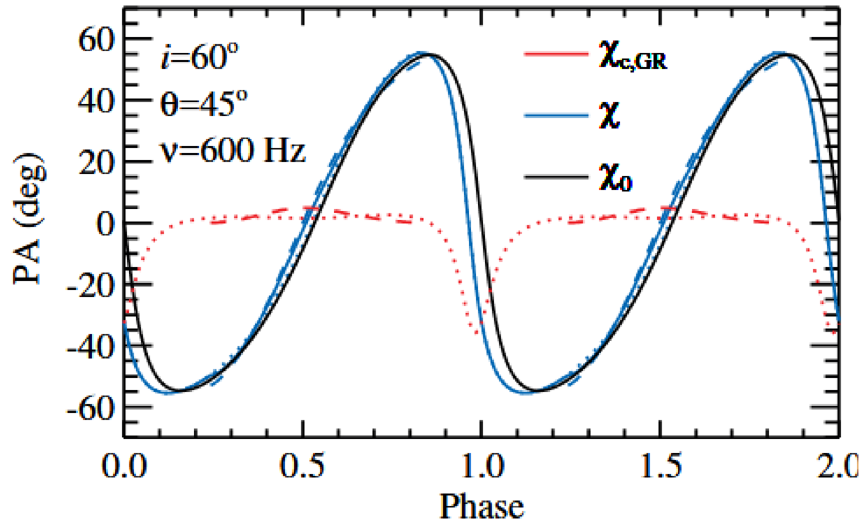

Poutanen (2020)

RVM in magnetars – 4U 0142+61

- BB+PL – thermal emission (condensed surface) + magnetospheric RCS

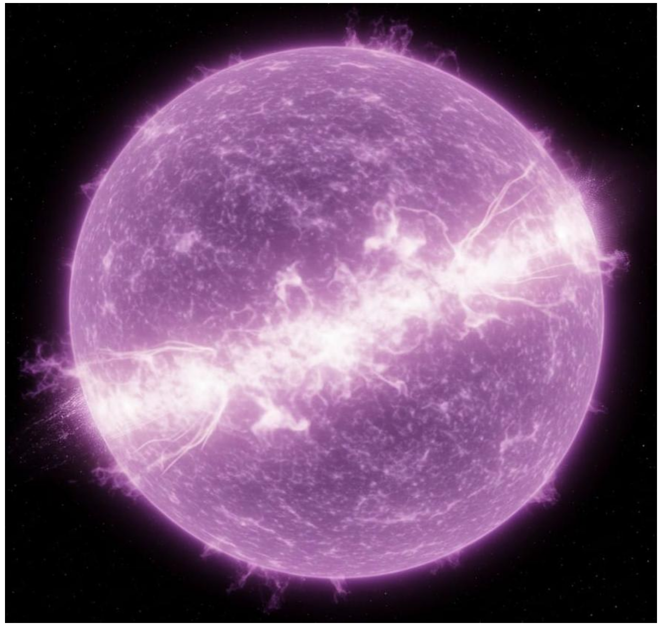

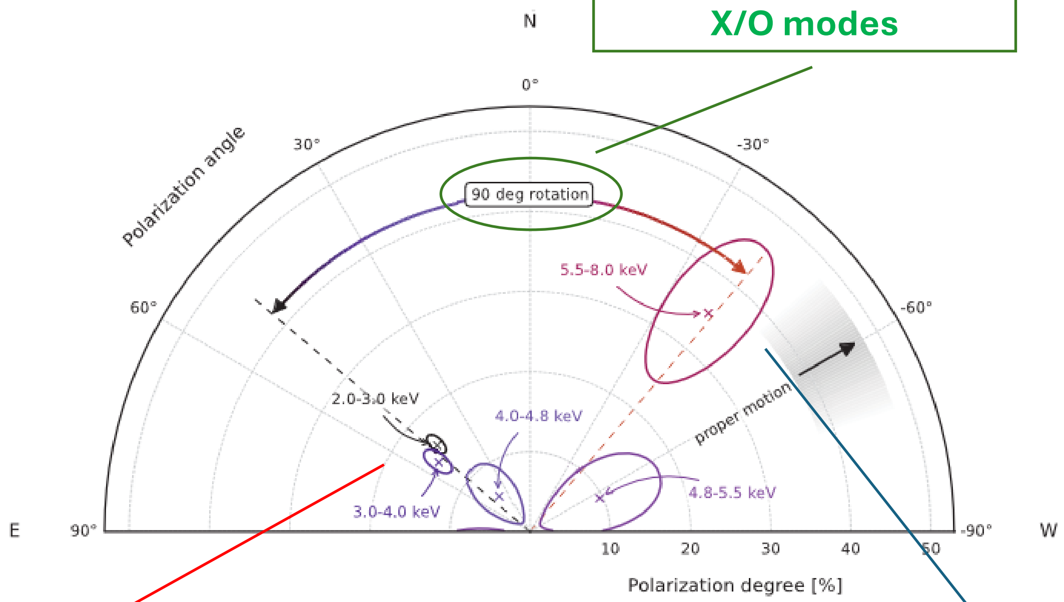

90° swing
X/O modes

Low energies (2–4 keV)
PD ≈ 15% – PA ≈ 50°
Condensed surface

High energies (6–8 keV)
PD ≈ 35% – PA ≈ −40°
RCS

Taverna et al. (2022)

RVM in magnetars – 4U 0142+61

- Phase-dependent PD coherent with the LC (double-peaked and in-phase)
  → <u>determined at the surface</u>

- Phase-dependent PA uncorrelated with the LC (single-peaked, quasi-sinusoidal – RVM)
  → <u>rotating vector model</u>

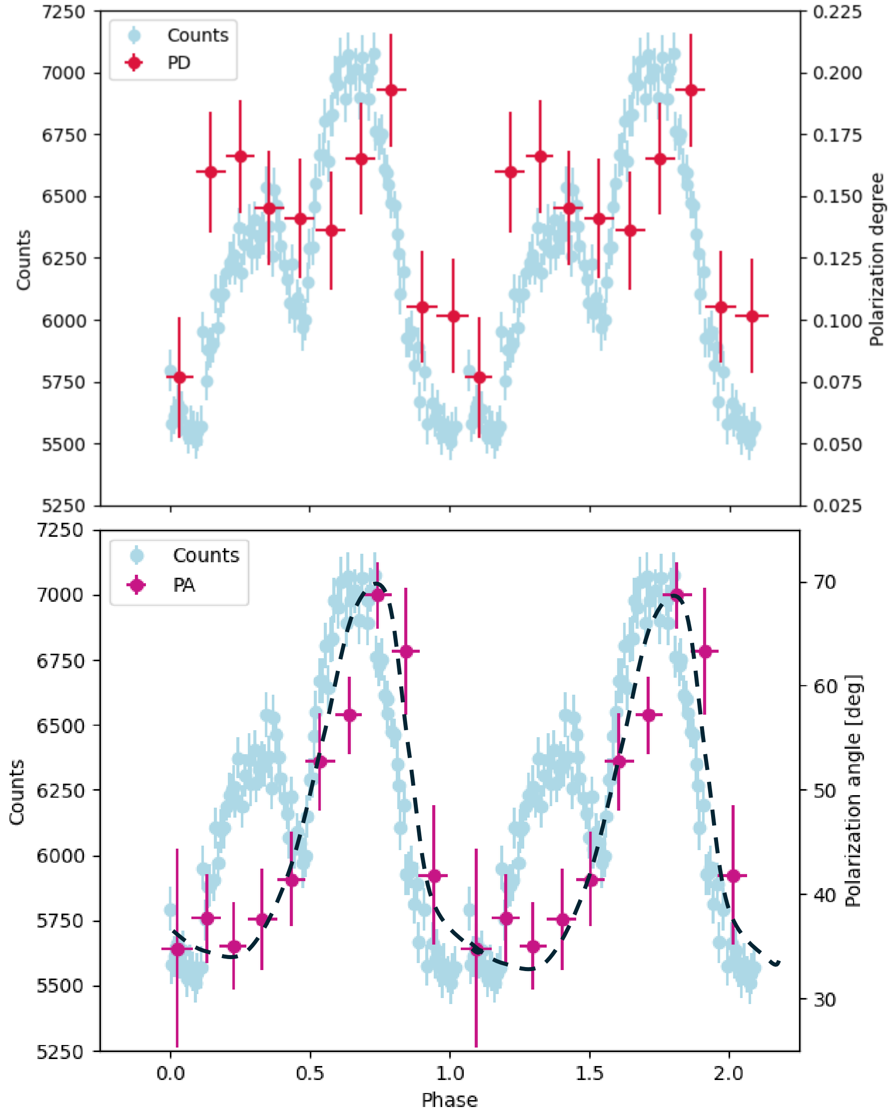

RVM in magnetars – 1RXS J1708

- BB+BB – two thermally emitting regions

- Phase-transition across the surface
  - Hotter ⇒ Magnetized atmosphere (high PD)
  - Colder ⇒ Condensed surface (low PD)

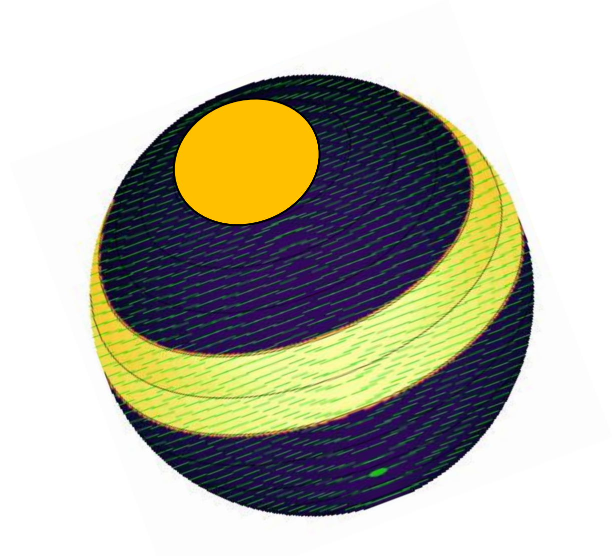

Cap + Belt

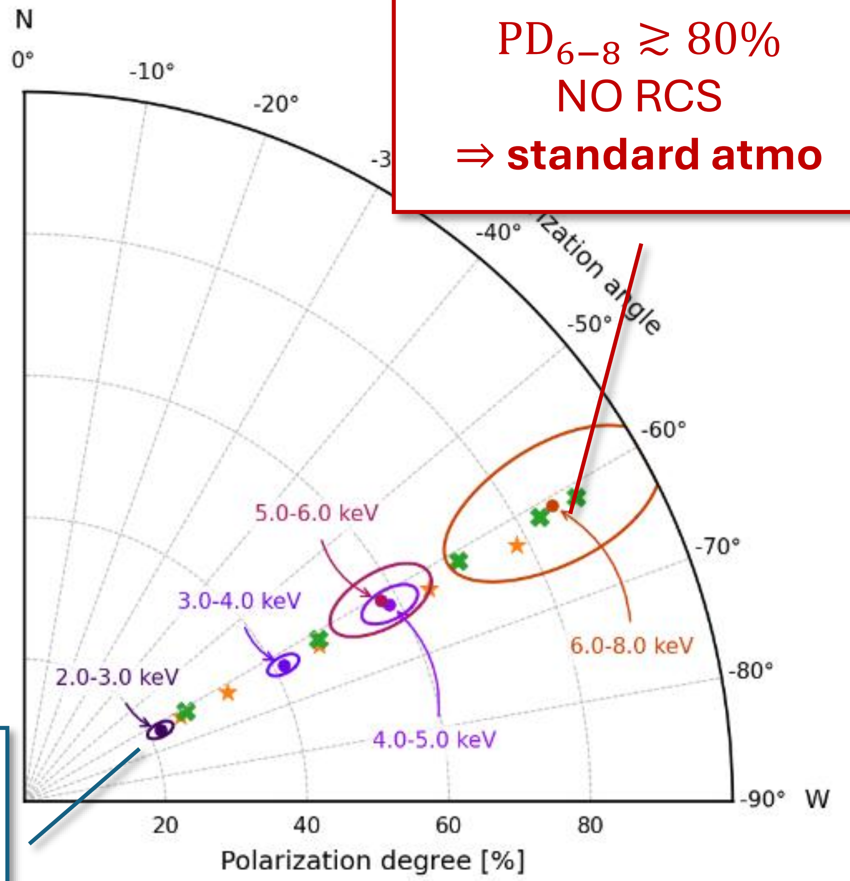

Zane et al. (2023)

$PD_{6-8} \gtrsim 80\%$
NO RCS
⇒ **standard atmo**

$PD_{2-4} \lesssim 40\%$
NO atmo
⇒ **condensed surface**

RVM in magnetars – 1RXS J1708

- Phase-dependent polarization analysis

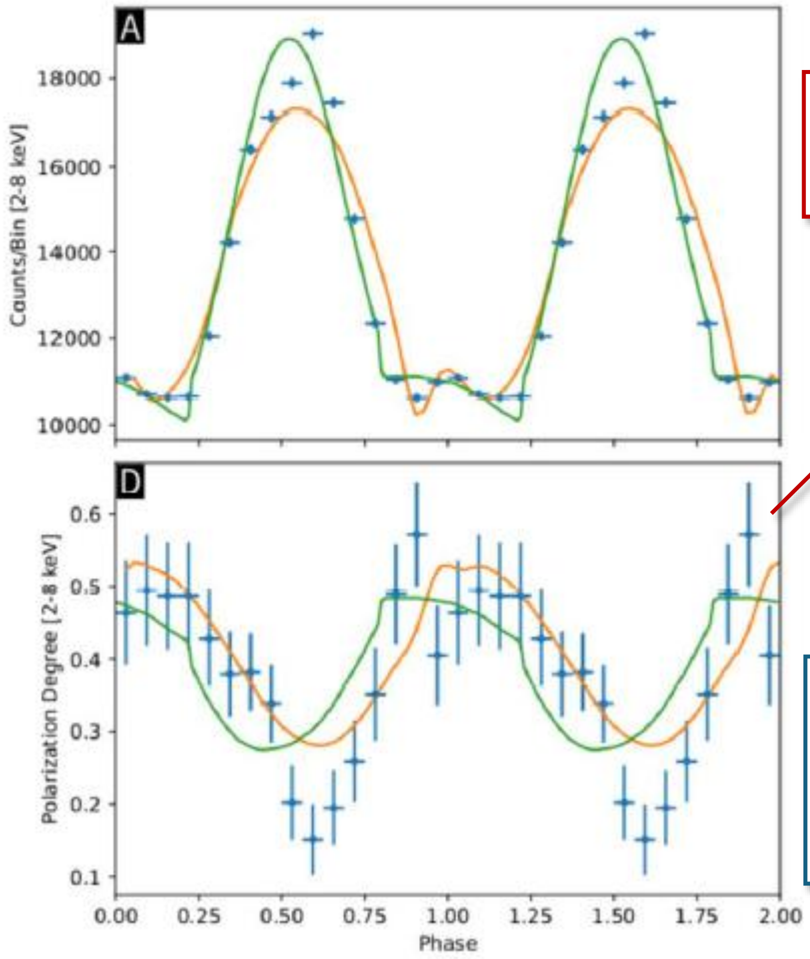

PD in counter-phase with the lightcurve

PA still display an oscillatory behavior consistent with RVM

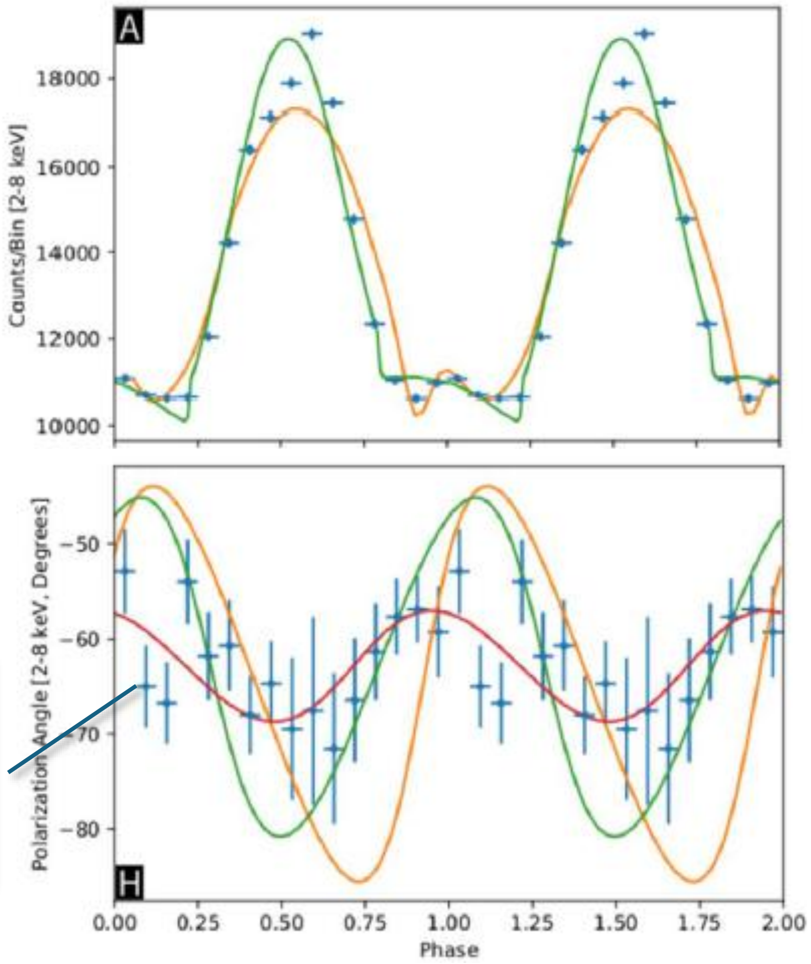

Zane et al. (2023)

RVM in magnetars – 1E 2259+586

- BB+PL+Absorption line – Proton cyclotron feature

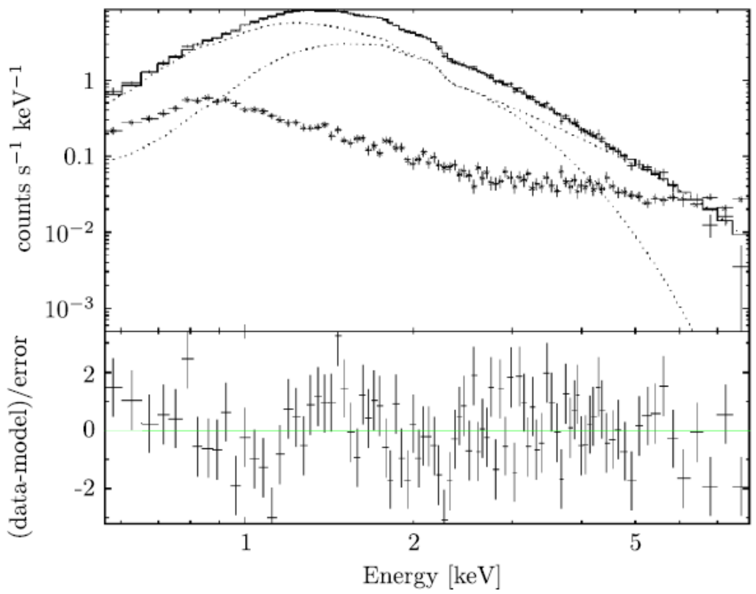

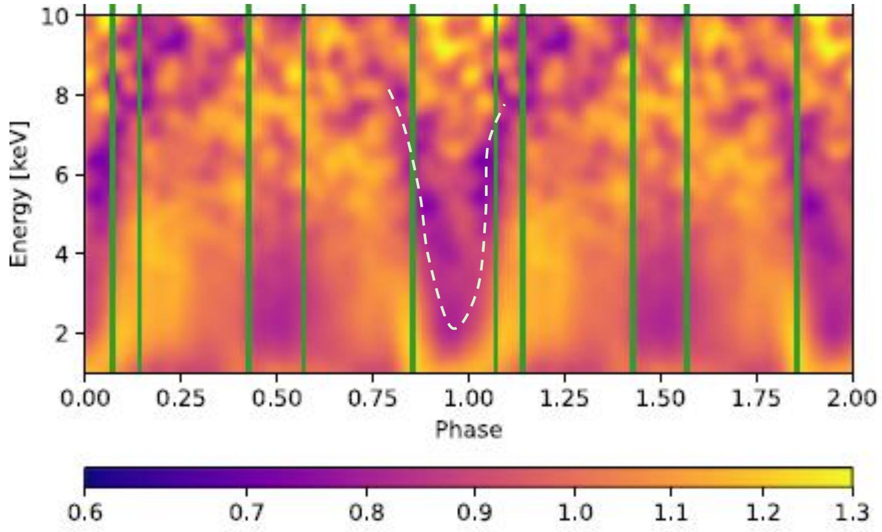

Data	N_H (10^{22} cm^{-2})	kT_{BB} (keV)	R_{BB} [a] (km)	Γ_{PL}	Norm$_{PL}$ at 1 keV (10^{-3} s^{-1} keV^{-1}cm^{-2})	E_{abs} (keV)	σ_{abs} (keV)	Depth$_{abs}$ (keV)	χ^2/dof
PN + MOS	$0.91^{+0.08}_{-0.13}$	$0.446^{+0.008}_{-0.009}$	$2.24^{+0.13}_{-0.13}$	$3.93^{+0.08}_{-0.11}$	$50.72^{+6.87}_{-9.14}$	$0.71\pm^{+0.17}_{-0.22}$	$0.30^{+0.09}_{-0.08}$	$0.30^{+0.63}_{-0.20}$	341.0/245
PN	$1.02^{+0.03}_{-0.07}$	$0.437^{+0.012}_{-0.011}$	$2.33^{+0.22}_{-0.21}$	$4.09^{+0.08}_{-0.08}$	$62.09^{+6.81}_{-6.41}$	$0.96^{+0.07}_{-0.18}$	$0.23^{+0.10}_{-0.06}$	$0.11^{+0.20}_{-0.05}$	94.1/93
IXPE [b]	1.02 [c]	$0.429^{+0.011}_{-0.010}$	$2.45^{+0.24}_{-0.20}$	$4.36^{+0.09}_{-0.09}$	$75.95^{+7.79}_{-7.80}$	0.96 [c]	0.23 [c]	0.11 [c]	138.0/147

Heyl et al. (2024)

RVM in magnetars – 1E 2259+586

- Peculiar phase-dependent behavior
  - Two antipodal condensed-surface spots (one covered by the loop)

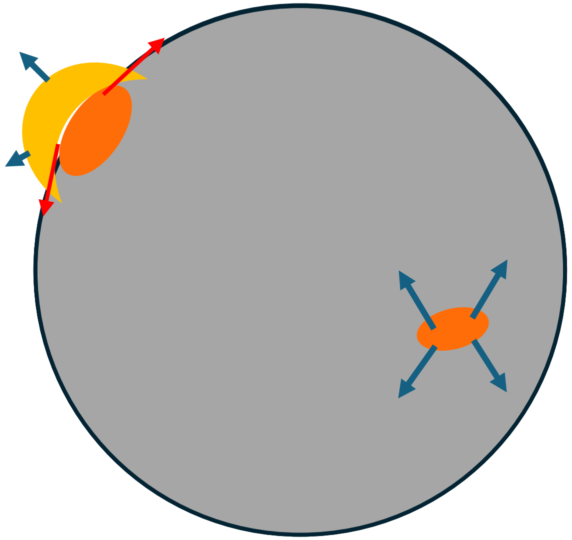

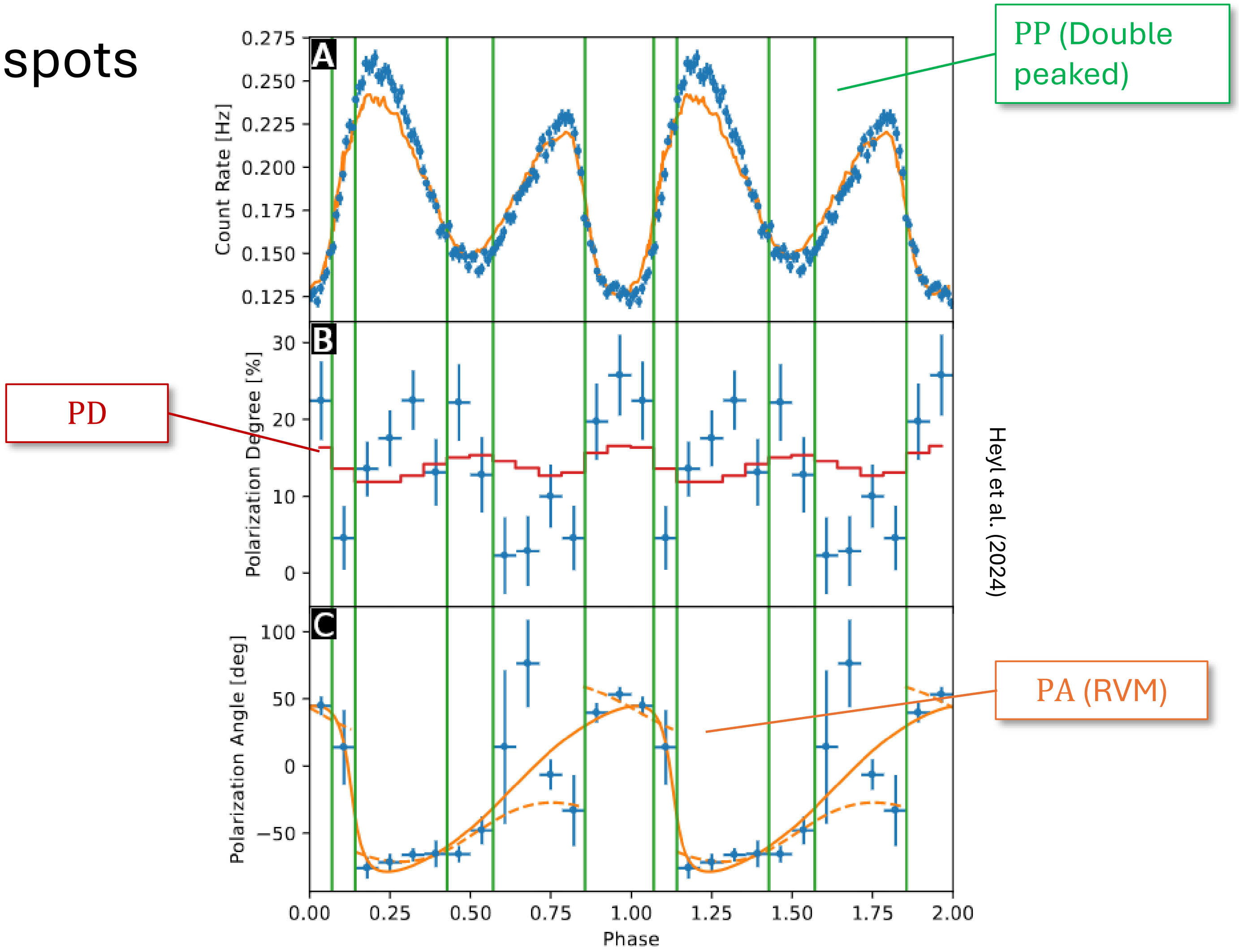

RVM in magnetars – 1E 1547–5408

- Radio-loud magnetar (single BB in X-rays, typical pulse in radio)
- PA still follows the RVM predictions

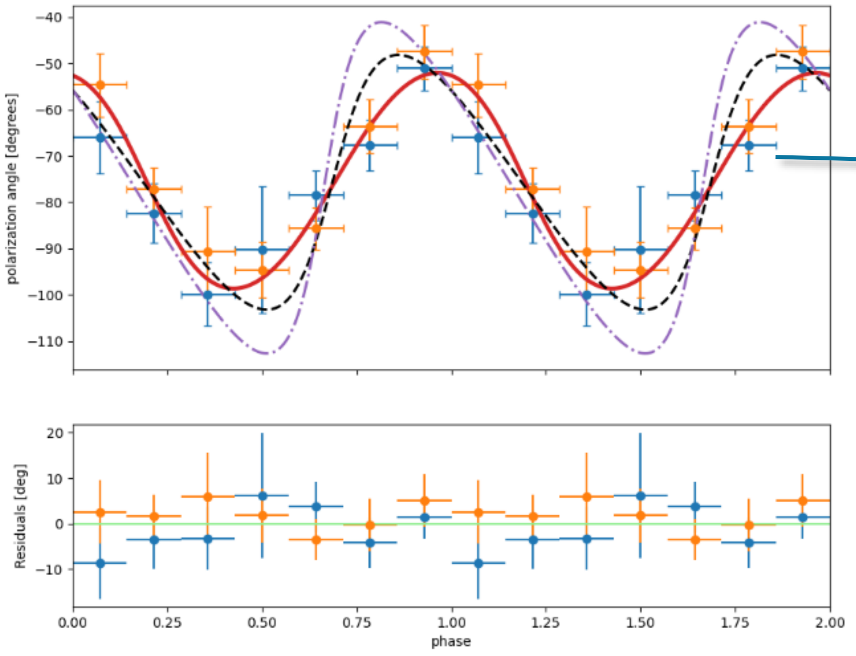

Taverna et al. (2026, *submitted*)

X-rays

radio

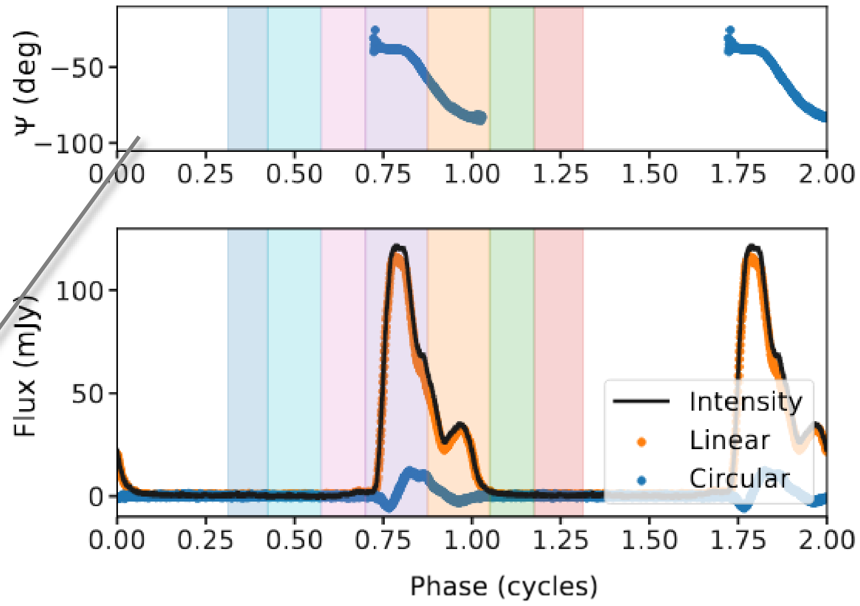

Stewart et al. (2025, *submitted*)

RVM in magnetars – 1E 1547–5408

- Radio-loud magnetar (single BB in X-rays, typical pulse in radio)
- PA still follows the RVM predictions

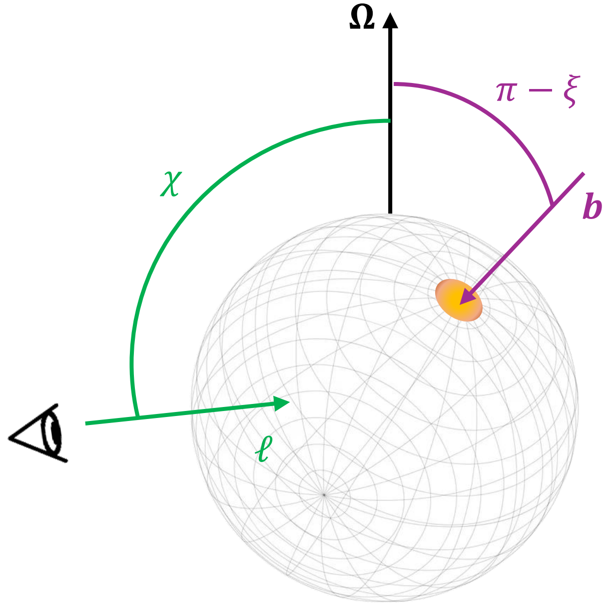

$\chi \approx 97°$
$\xi \approx 160°$

Taverna et al. (2026, *submitted*)

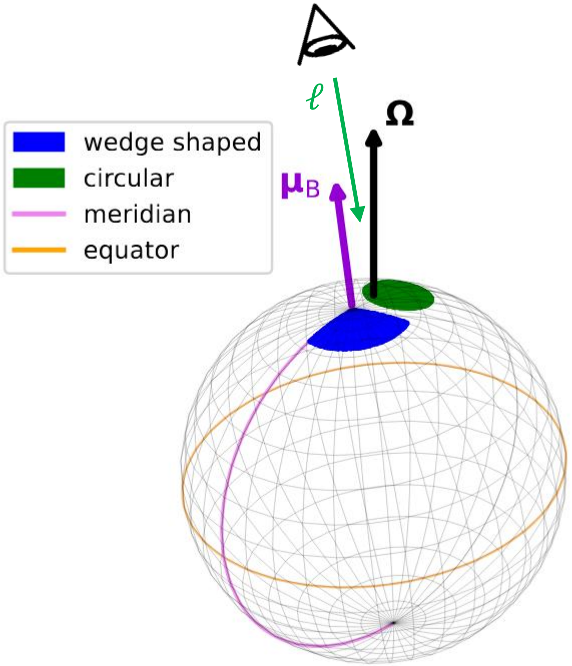

$\chi \approx 2°$
$\xi \approx 5°$

Stewart et al. (2025, *submitted*)

RVM in magnetars – Others

- No sufficient statistics for a significant phase-dependent analysis for SGR 1806–20 and AXP 1E 1841–045
- Low polarization detected in 1806 is difficult to achieve with IXPE $\Rightarrow$ new possibilities with eXTP and EXPO
- New observation scheduled for 1E 1841 (during IXPE GO-3)

$$t_{\rm exp} \quad 300 \ \rightarrow \ 700 \ {\rm ks}$$

RVM in magnetars

- In all magnetars observed (with enough statistics) PA follows the RVM (regardless of the complexity of phase-dependent PD and of PP)
- Emission mechanisms in magnetars are different from pulsars (thermal, RCS, almost isotropic…)
- Much more complex magnetic field topology (twisted fields, local structures)
- Variety of emission geometries

RVM in magnetars

- In a
  (reg
- Em … al,
  RC
- Mu
  str
- Var

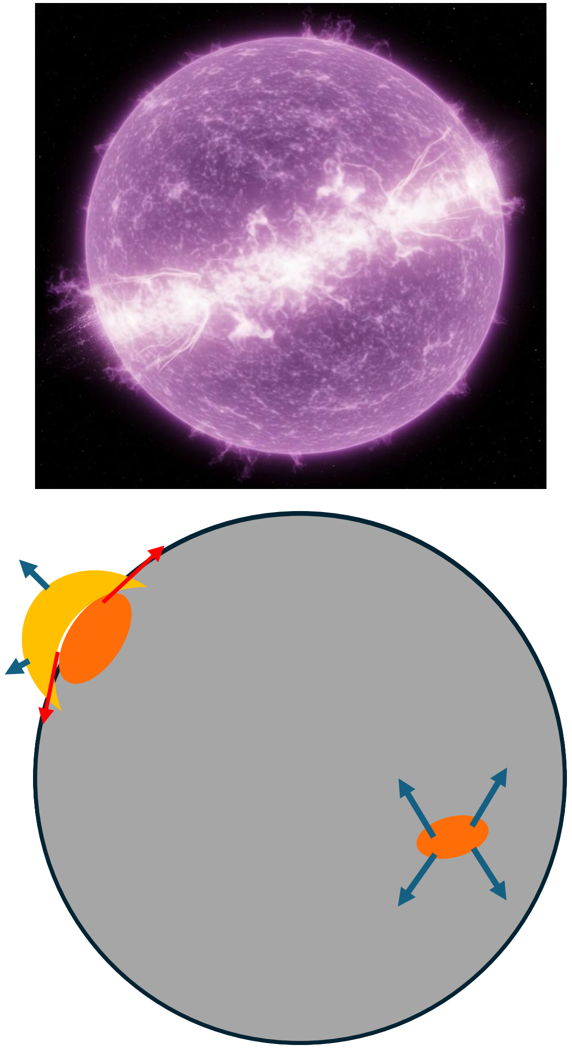

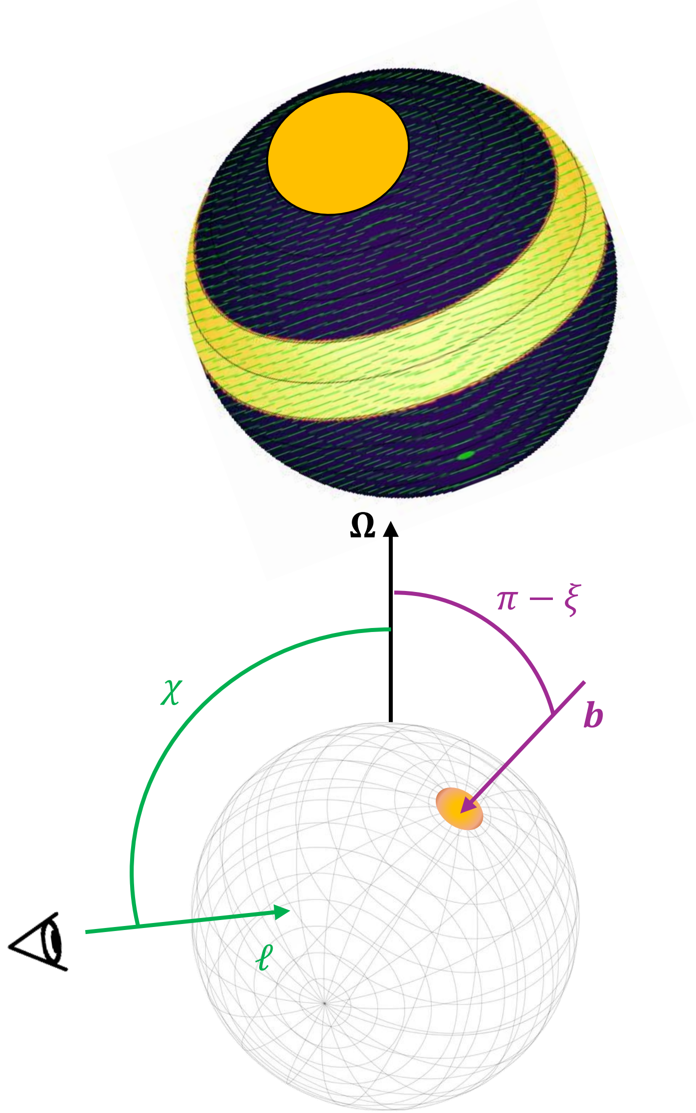

RVM in magnetars

- In all magnetars observed (with enough statistics) PA follows the RVM (regardless of the complexity of phase-dependent PD and of PP)
- Emission mechanisms in magnetars are different from pulsars (thermal, RCS, almost isotropic…)
- Much more complex magnetic field topology (twisted fields, local structures)
- Variety of emission geometries

Why should we observe the RVM in magnetars?

$\boldsymbol{E}$-$\boldsymbol{b}$ alignment

- Differently from curvature radiation, rays along the LOS may form any angle with respect to the local $\boldsymbol{B}$-field

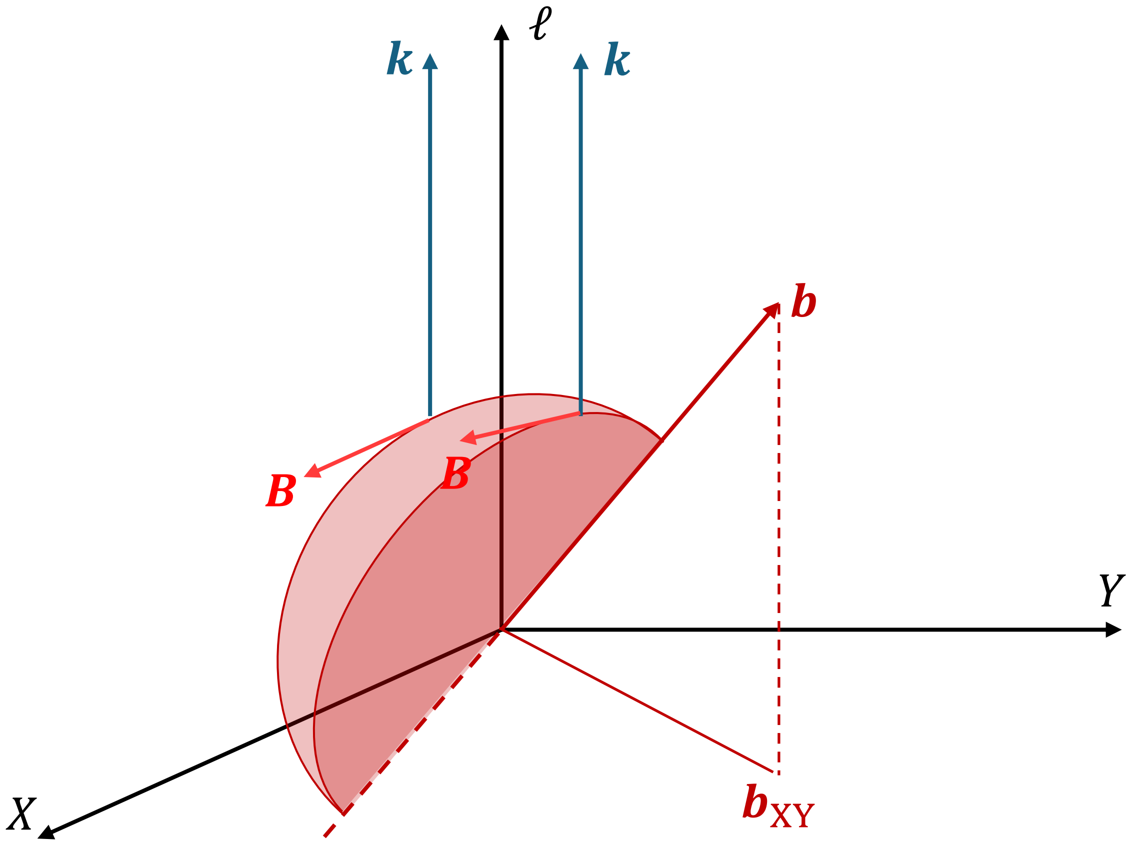

- Polarization vectors $\boldsymbol{E}$ are not constrained anymore to lie in the plane of the field line
- No law which relates intensity with θ

The (average) vectorial sum of the $\boldsymbol{E}$-vector projections is in general not aligned with $\boldsymbol{b}_{\mathrm{XY}}$

$\boldsymbol{E}$-$\boldsymbol{b}$ alignment

- Differently from curvature radiation, rays along the LOS may form any angle with respect to the local $\boldsymbol{B}$-field
- For B in excess of B_{QED}, photons turn out to be polarized linearly and only in two normal modes

$$\hat{\boldsymbol{E}} = \begin{pmatrix} 1 \\ 0 \\ 0 \end{pmatrix} \quad \text{or} \quad \begin{pmatrix} 0 \\ 1 \\ 0 \end{pmatrix}$$

Ordinary mode **Extraordinary mode**

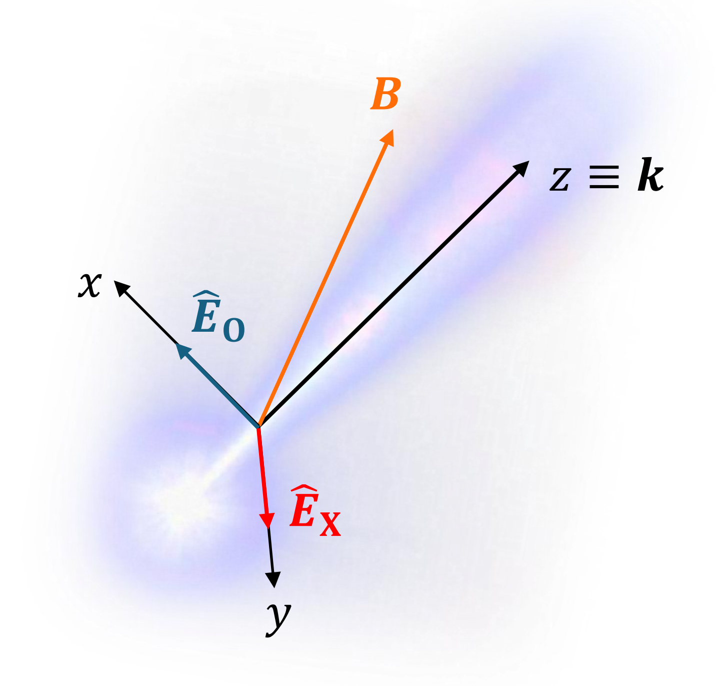

Polarization vectors directly anchored to the magnetic field topology.

E, b alignment

- D
  ar
- Fo ly
  in

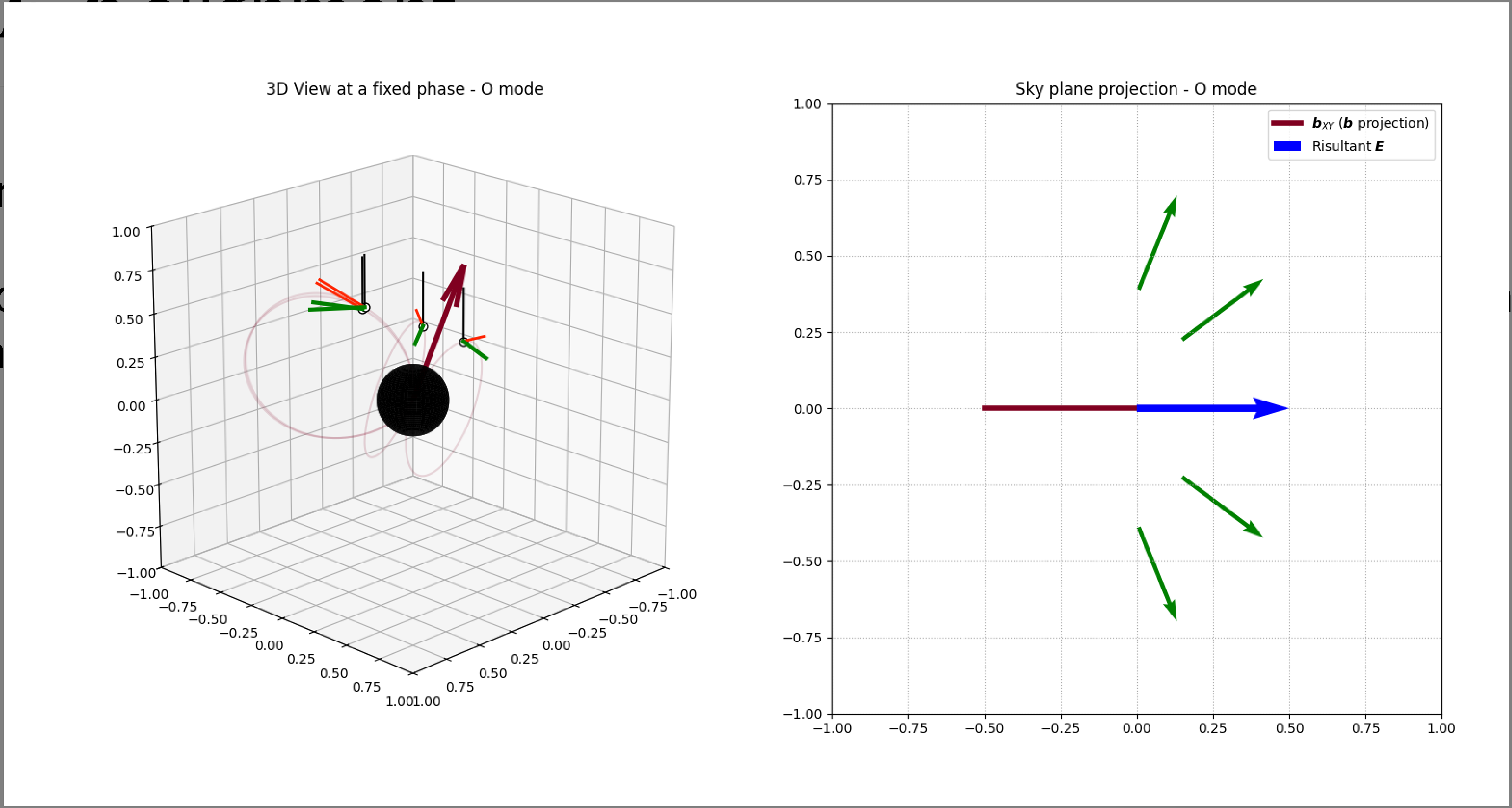

topology.

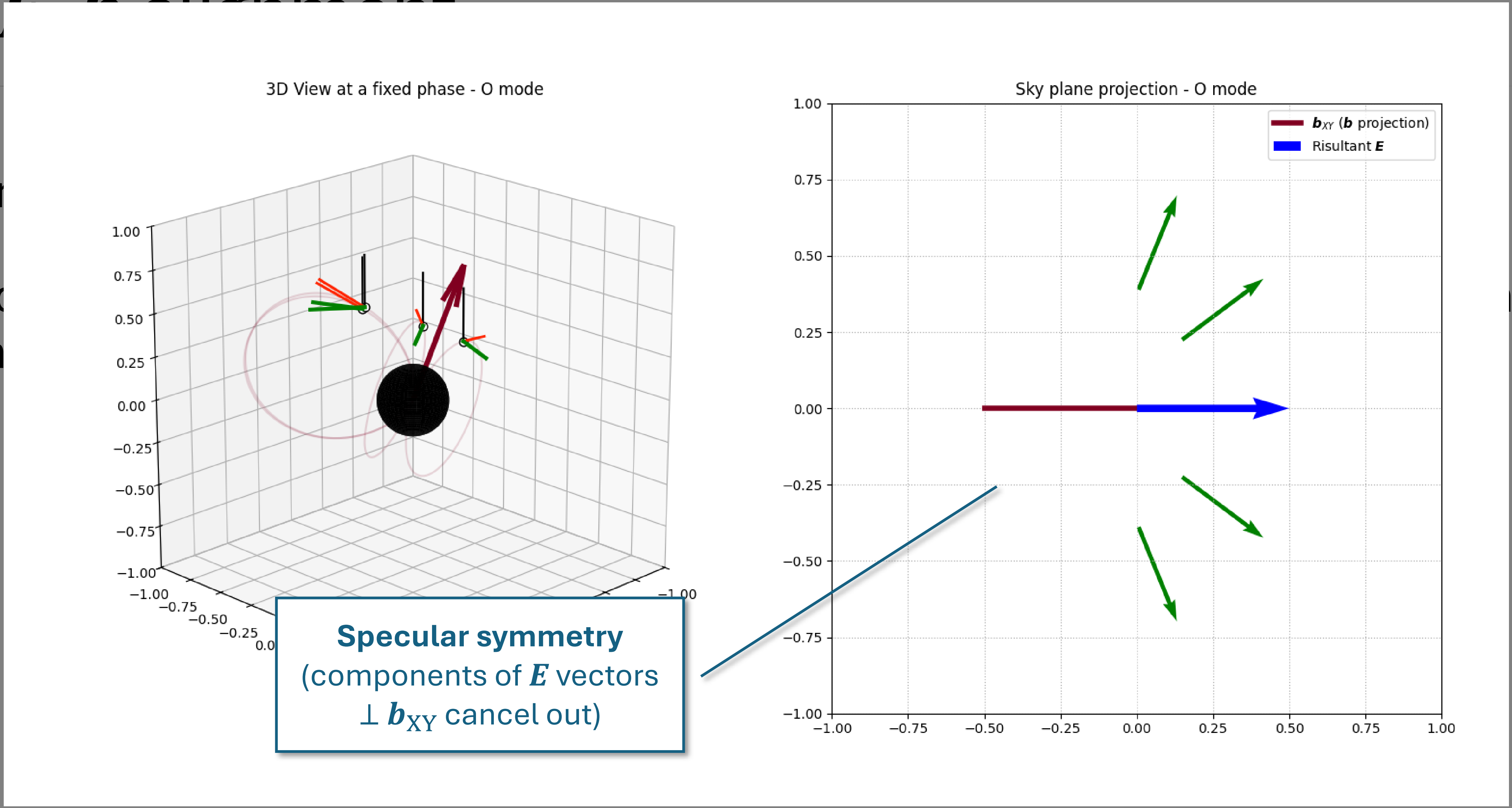
3D View at a fixed phase - O mode
Sky plane projection - O mode
b_{XY} (b projection)
Risultant E
Specular symmetry
(components of E vectors $\perp b_{XY}$ cancel out)

topology.

E–b alignment

- D… ar…
- Fo… in… …ly

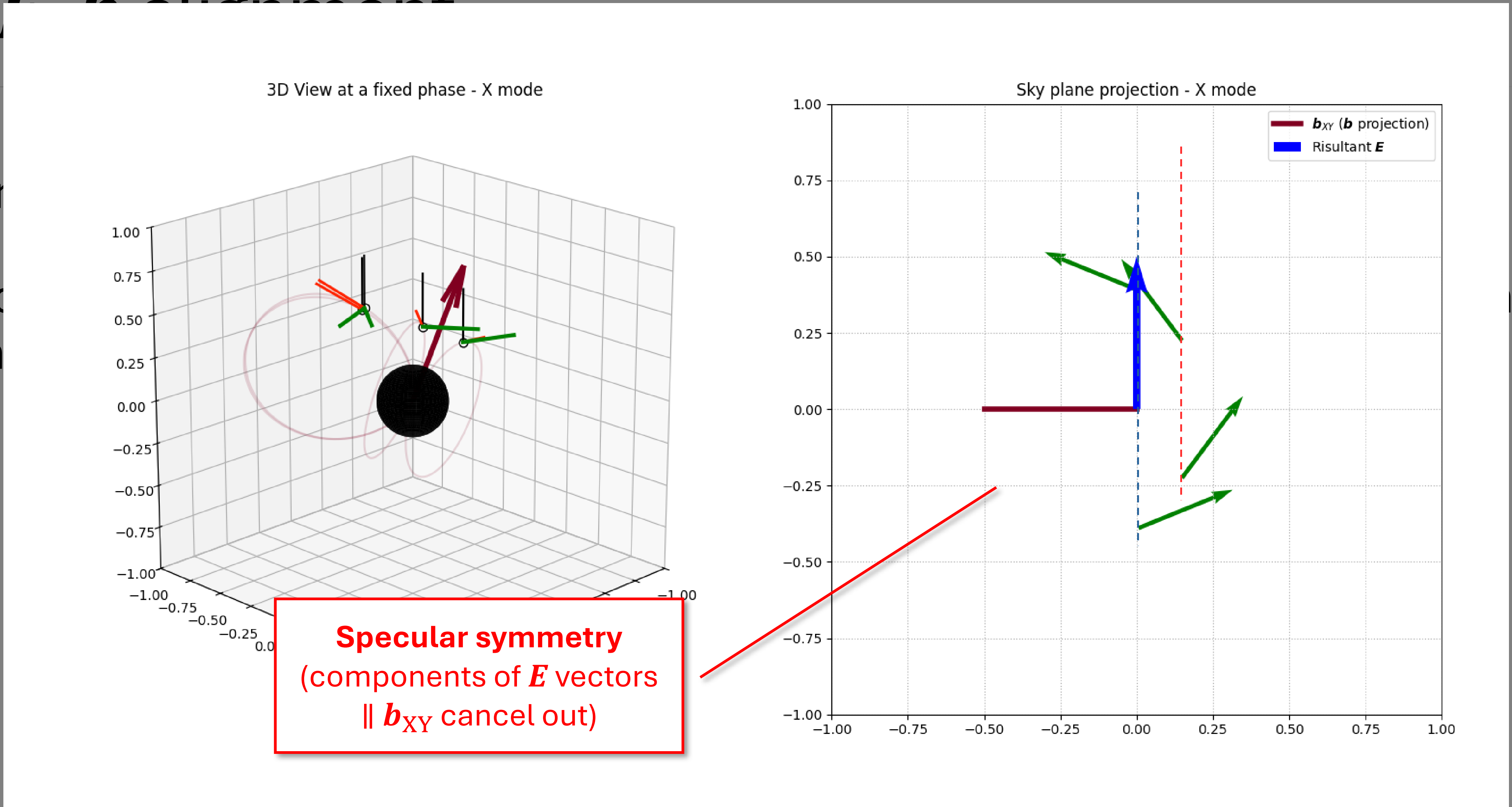

topology.

$\boldsymbol{E}$-$\boldsymbol{b}$ alignment

- Differently from curvature radiation, rays along the LOS may form any angle with respect to the local $\boldsymbol{B}$-field

- For B in excess of B_{QED}, photons turn out to be polarized linearly and only in two normal modes

- Two rotating vectors in the sky plane
  - $\boldsymbol{b}_{\mathrm{XY}}$ for O-mode photons
  - the orthogonal to $\boldsymbol{b}_{\mathrm{XY}}$ for X-mode photons

PA oscillation according to the usual law (possibly offset by 90°)

Symmetry requirement

- To ensure the extinction of non-parallel (non-perpendicular) components, in the sky plane, $\boldsymbol{E}$-vectors must be **pairwise**, mirroring each other across (parallel to) the projected magnetic dipole
- This requires an **emission region symmetric with respect to $\boldsymbol{b}$...**

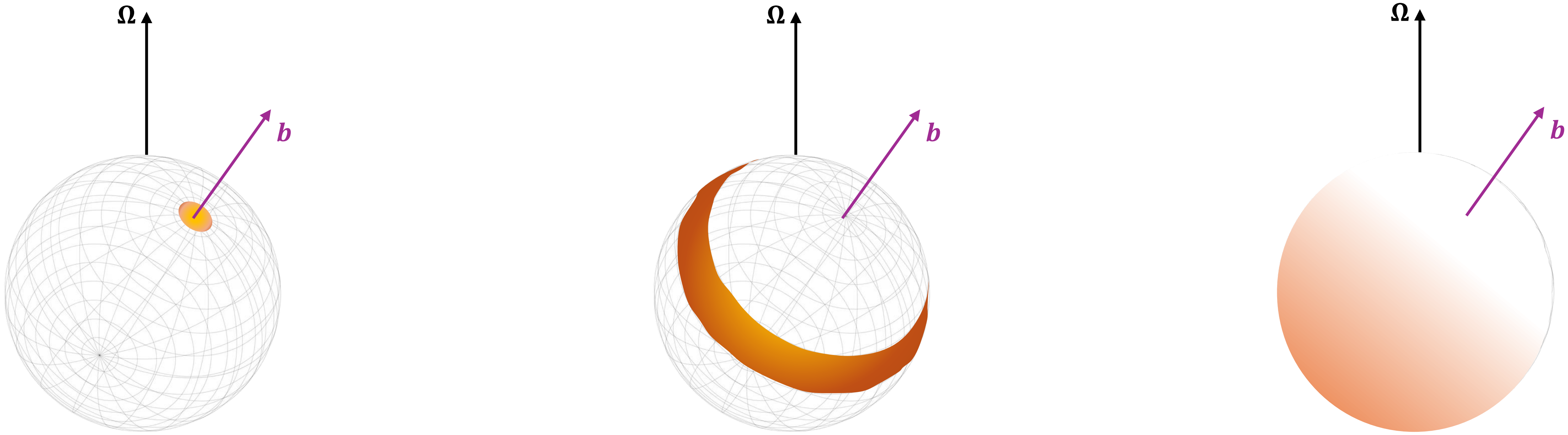

Symmetry requirement

- To ensure the extinction of non-parallel (non-perpendicular) components, in the sky plane, $\boldsymbol{E}$-vectors must be **pairwise**, mirroring each other across (parallel to) the projected magnetic dipole
- This requires an **emission region symmetric with respect to $\boldsymbol{b}$**
- ...and **also with respect to ℓ** ($\boldsymbol{E}$-vectors must appear in the sky plane)

Asymmetric emitting regions

- In case of emitting regions not symmetric wrt the magnetic axis cancellation does not occur and the resultant E would be misaligned from $\boldsymbol{b}$ (or $90°$-$\boldsymbol{b}$)

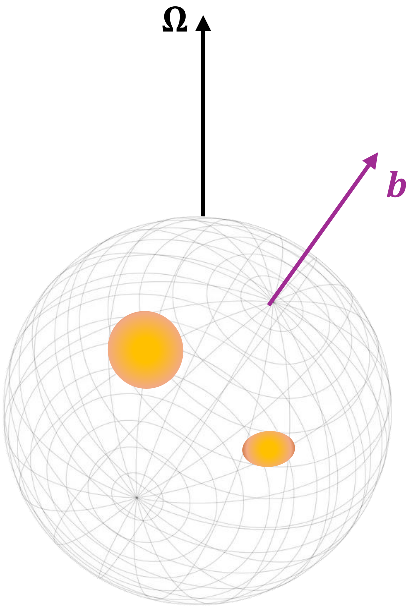

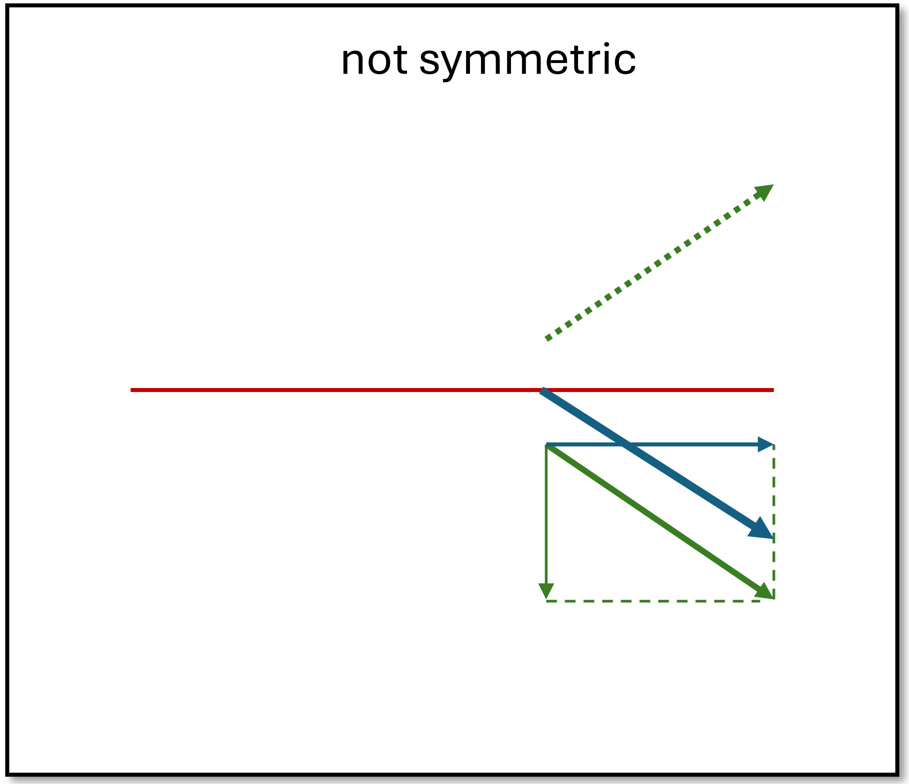

Asymmetric emitting regions

- In case of emitting regions not symmetric wrt the magnetic axis cancellation does not occur and the resultant E would be misaligned from $\boldsymbol{b}$ (or $90°$-$\boldsymbol{b}$)

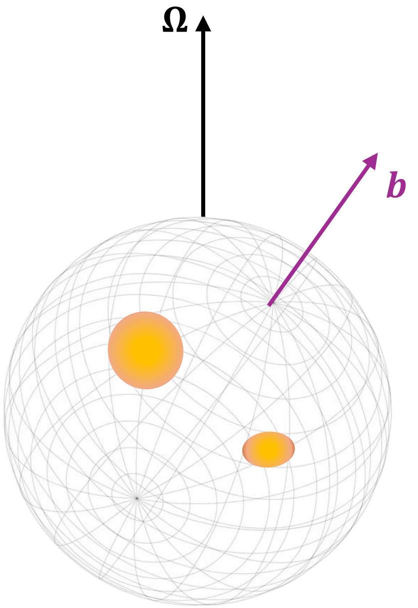

PA still follows the RVM, provided that the emitting regions remain fixed on the surface

A change in shape may be revealed in a change in the PA phase-oscillation

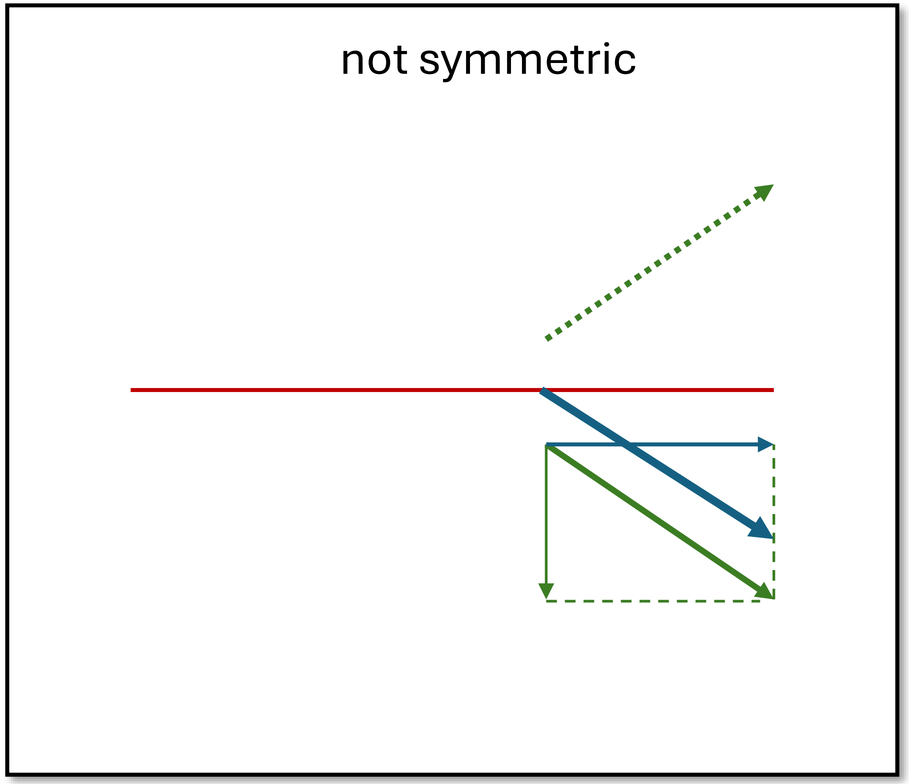

Magnetic field topology

- The RVM relies on a dipolar topology (axis-symmetric, field lines in the meridional plane, …)

- Magnetar surface fields are expected to be much more complex…

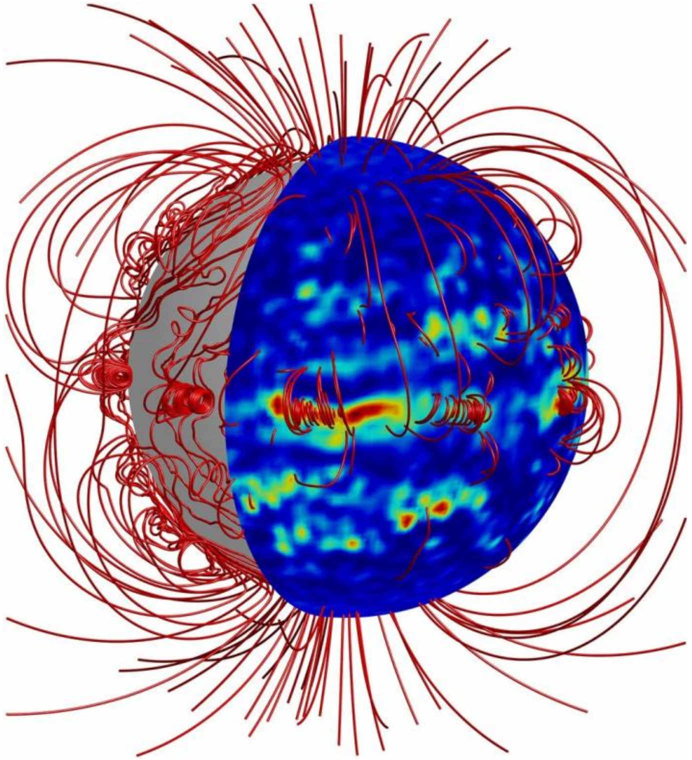

Gourgouliatos et al. (2016)

← … dipolar shape recovered at large distances

Magnetic field topology

- The RVM relies on a dipolar topology (axis-symmetric, field lines in the meridional plane, ...)
- Magnetar surface fields are expected to be much more complex...
- If the observed PA in magnetars follows the RVM, the «polarization topology» must be fixed far from the surface

⇓

Vacuum polarization

Transport of polarization at infinity $B \gtrsim B_{\mathrm{QED}}$

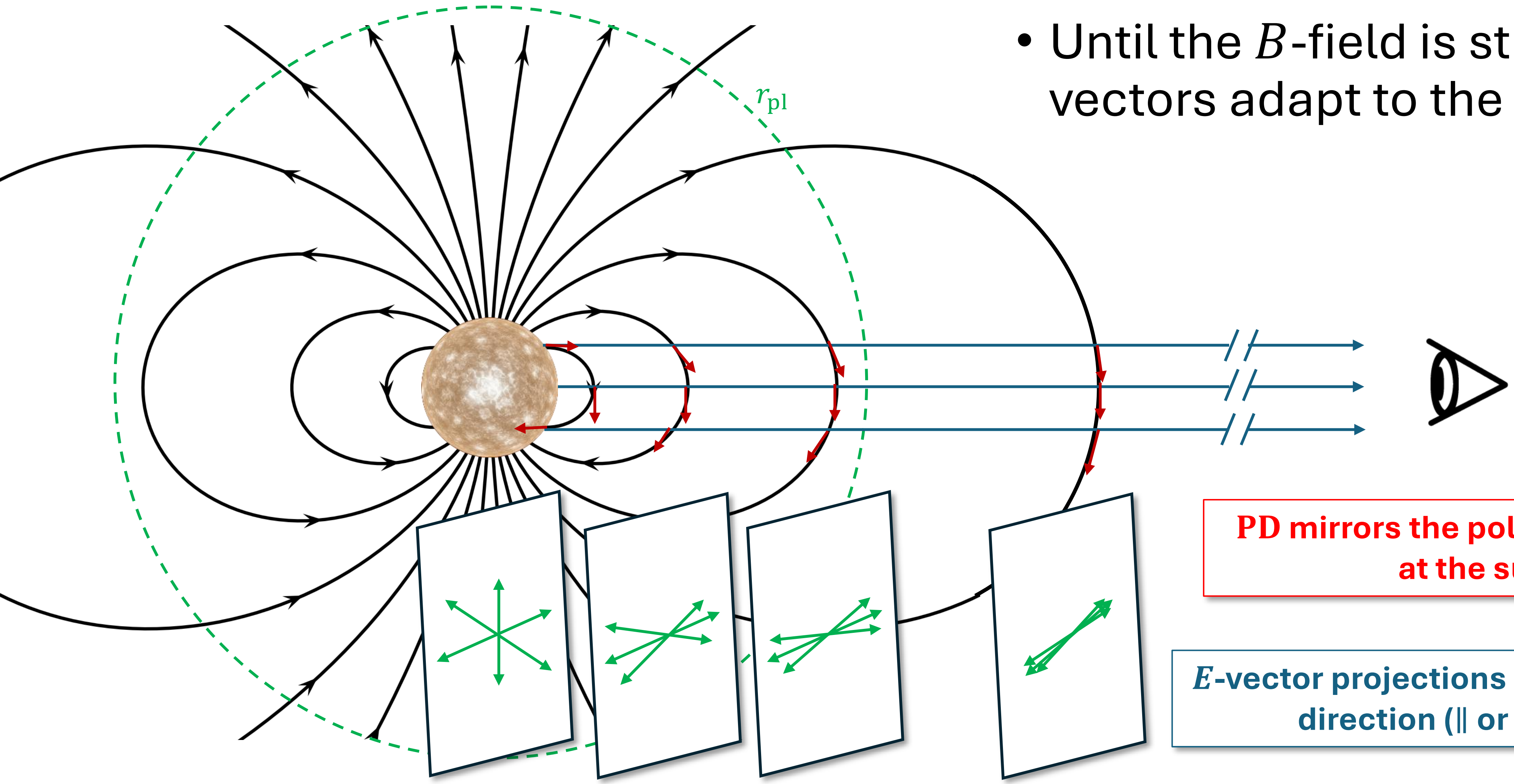

- Until the B-field is strong the $\boldsymbol{E}$-vectors adapt to the local $\boldsymbol{B}$

PD mirrors the polarization pattern at the surface

$\boldsymbol{E}$-vector projections align to a single direction (∥ or ⊥ to $\boldsymbol{b}_{\mathrm{XY}}$)

Transport of polarization at infinity $B \gtrsim B_{\mathrm{QED}}$

- Until the B-field is strong the $\boldsymbol{E}$-vectors adapt to the local $\boldsymbol{B}$

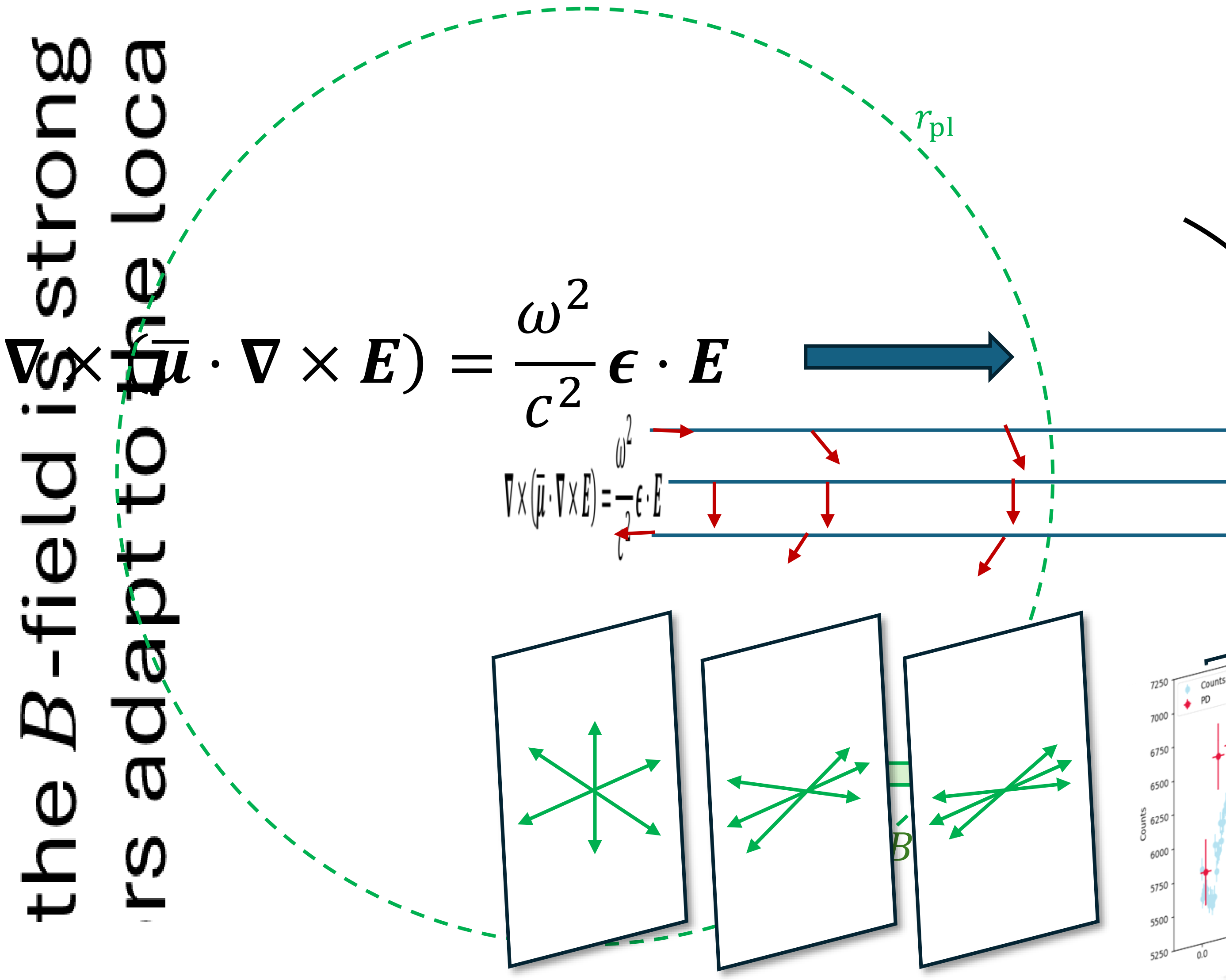

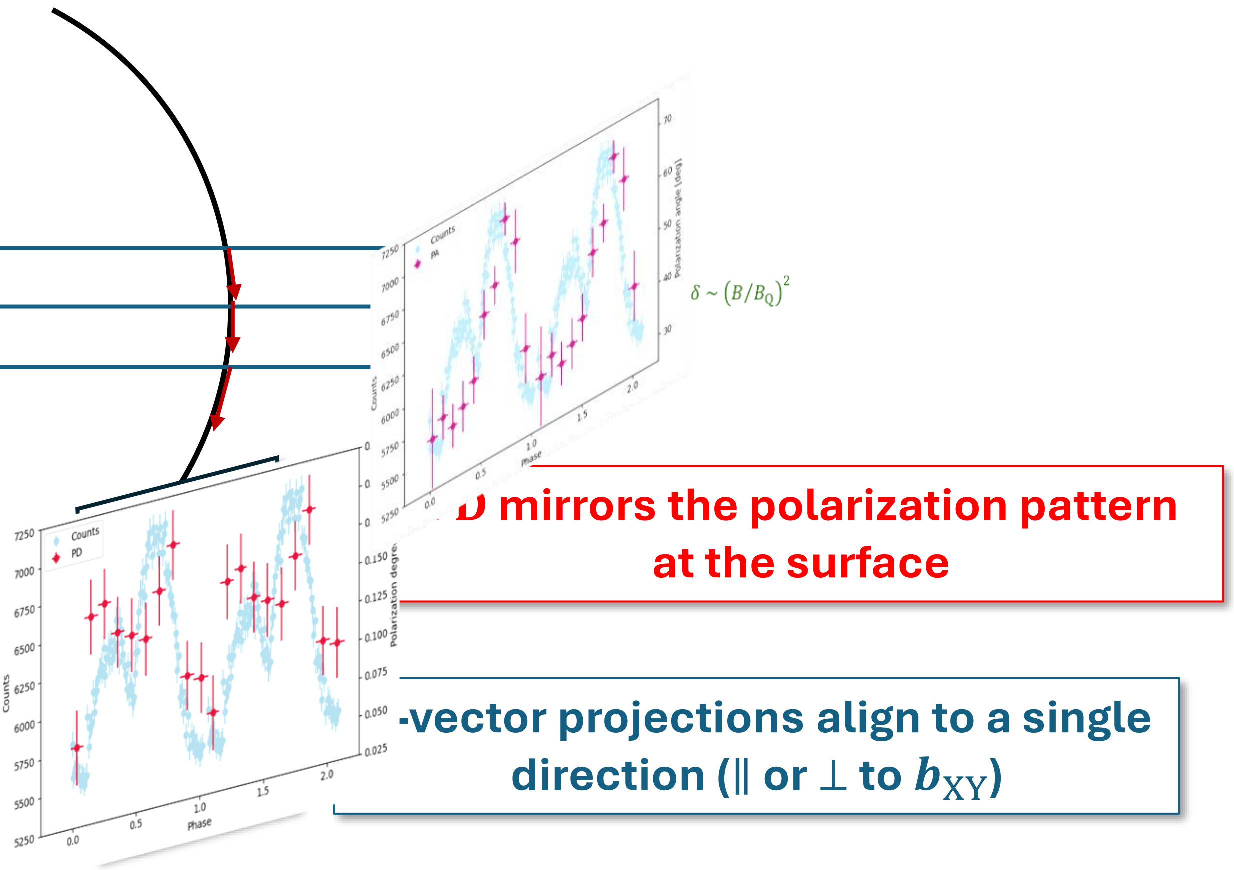

Vacuum birefringence and symmetry

- Beside ensuring a dipolar field topology, transport of polarization at $r_{\rm pl}$ tends to increase the degree of symmetry

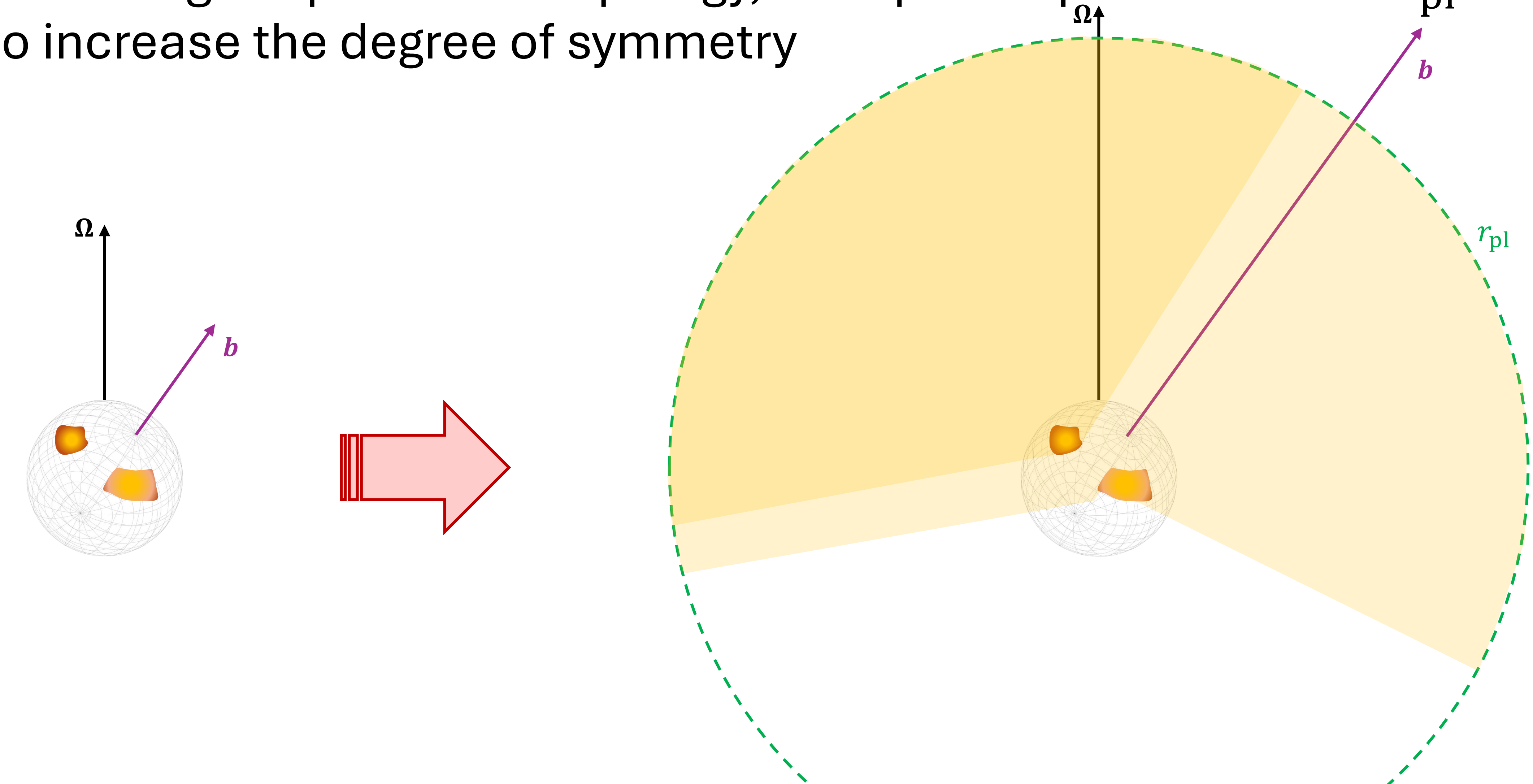

RVM and twisted fields

- According to the RCS scenario (Thompson et al. 2002), the external field may be a twisted dipole (maintaining the axial symmetry)

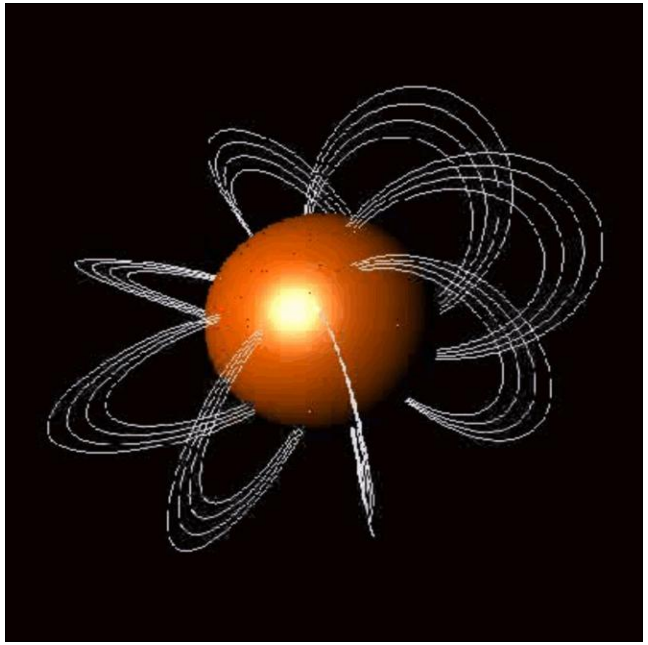

- This would break the meridional symmetry, causing the E-vector projection to misalign with respect to $\boldsymbol{b}_{\mathrm{XY}}$
- If the twist survives at large distances, this translates into a shift of the PA average value (proportional to the twist angle)

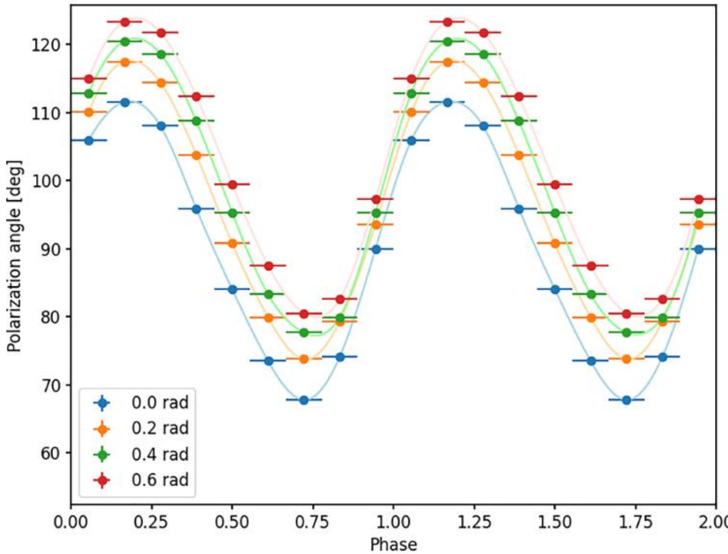

Ge et al. (2025)

RVM in different energy bands

- May these considerations explain the different geometries inferred for 1E 1547.0–5408 in the radio and in the X-ray bands?

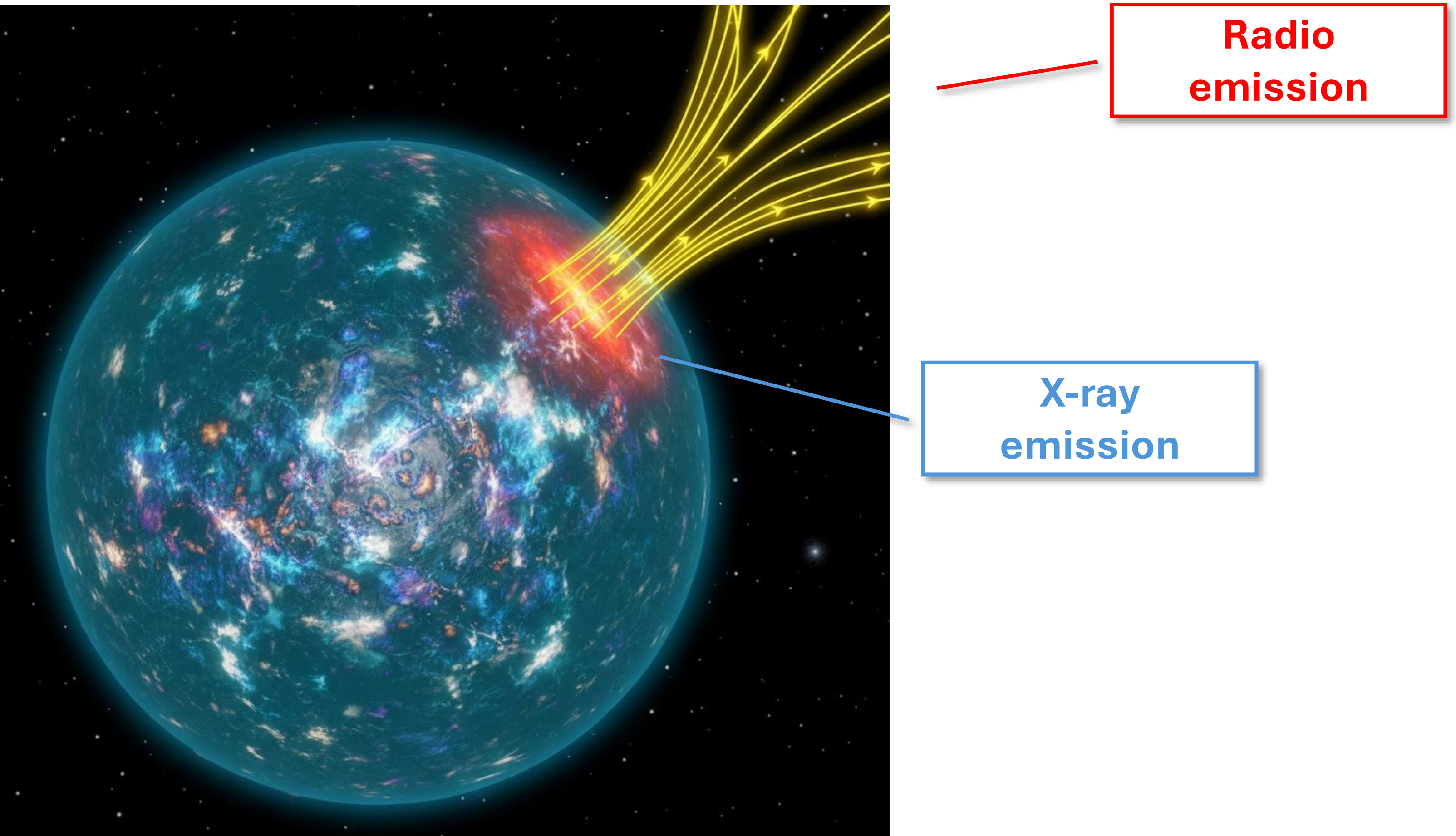

RVM in different energy bands

- May these considerations explain the different geometries inferred for 1E 1547.0–5408 in the radio and in the X-ray bands?

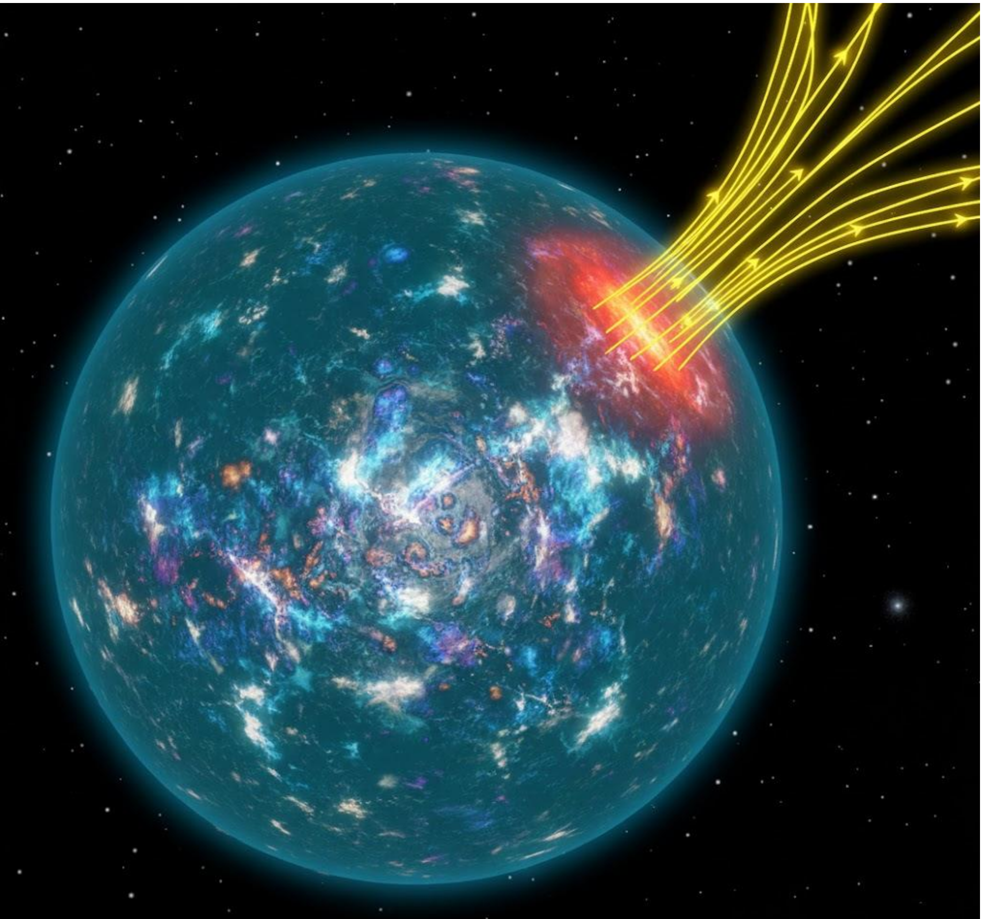

Radio – Parkes-Murriyang: $\sim$ 3.25 GHz

X-rays – IXPE: $\sim$ 4 keV

$$r_{\rm pl} \sim E^{1/5} B_{\rm p}^{2/5} \quad \Rightarrow \quad r_{\rm pl}^{\rm X} \approx 130\, R_{\rm NS}$$

$$r_{\rm em}^{\rm radio} \approx 30\, R_{\rm NS}$$

Is this sufficient to assume some difference in the conditions for RVM? (LOS/*b* symmetry, *B*-field topology...)

Conclusions and open questions

- A dipolar (or at least axis-symmetric) $\boldsymbol{B}$-field is required for PA to follow the RVM – May we infer deviations from the dipolar topology?
- Emission regions must be symmetric around $\boldsymbol{b}$ **and** around ℓ – Is it possible to constrain the emission model?
- Vacuum birefringence (O/X modes, transport of polarization at r_{pl}) is crucial to detect PA of magnetars following the RVM – How important is RVM for a vacuum birefringence test?
- RVM in different bands giving different geometries – Does this reflect the different symmetry properties at different distances? Is this suggesting different magnetic field topologies?

Quantitative calculations

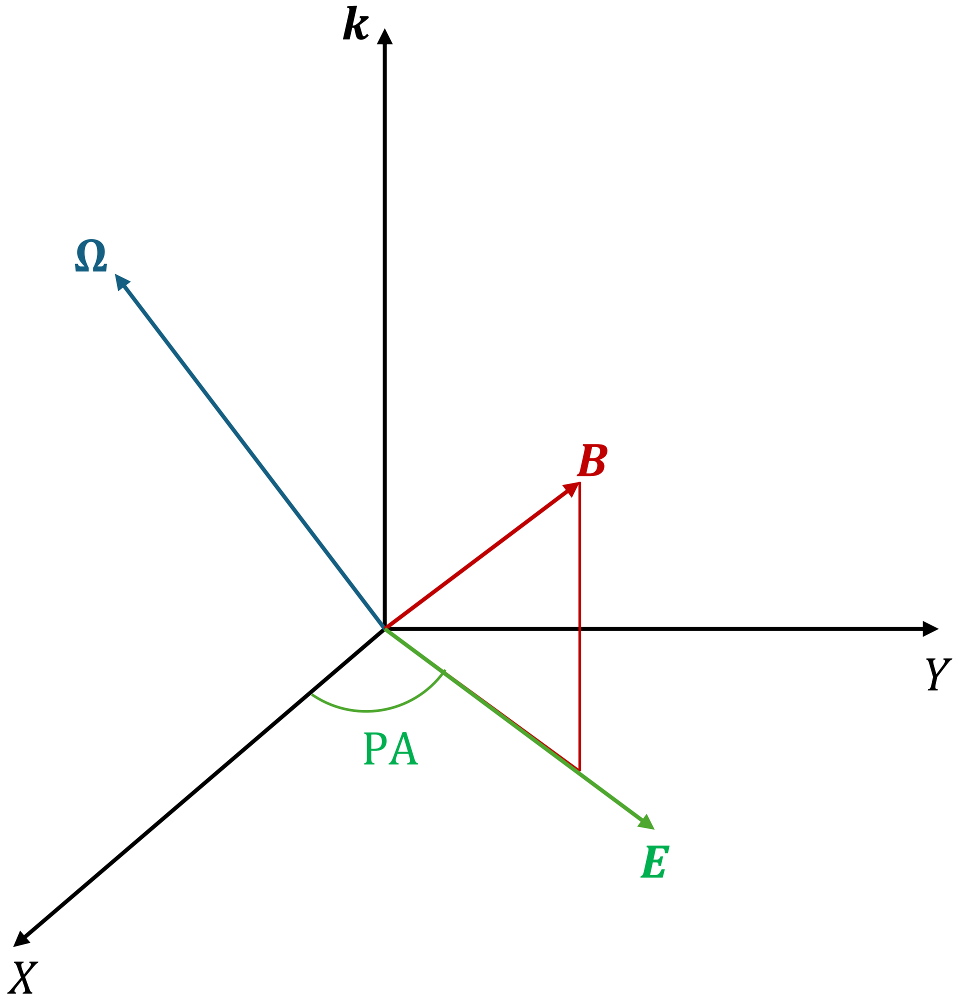

For **ordinary** photons, $\boldsymbol{E}$ is parallel to the projection of the local $\boldsymbol{B}$ field in the plane of the sky

In the (X, Y, Z) frame with $Z \parallel \ell$, if the local $\boldsymbol{B}$ has components

$$\boldsymbol{B} = \begin{pmatrix} B_X \\ B_Y \\ B_Z \end{pmatrix},$$

then the direction of $\boldsymbol{E}$ is given by

$$\boldsymbol{E} = \frac{\boldsymbol{B} - (\ell \cdot \boldsymbol{B})\ell}{|\boldsymbol{B} - (\ell \cdot \boldsymbol{B})\ell|} \quad \text{with} \quad \boldsymbol{B} - (\ell \cdot \boldsymbol{B})\ell = \begin{pmatrix} B_X \\ B_Y \\ 0 \end{pmatrix}.$$

Hence,

$$\boldsymbol{E} = \frac{1}{\sqrt{B_X^2 + B_Y^2}} \begin{pmatrix} B_X \\ B_Y \\ 0 \end{pmatrix}.$$

The position angle of $\boldsymbol{E}$ is then given by

$$\cos \mathrm{PA} = \boldsymbol{E} \cdot \boldsymbol{X} = \frac{B_X}{\sqrt{B_X^2 + B_Y^2}} \qquad \sin \mathrm{PA} = \boldsymbol{E} \cdot \boldsymbol{Y} = \frac{B_Y}{\sqrt{B_X^2 + B_Y^2}}$$

Quantitative calculations

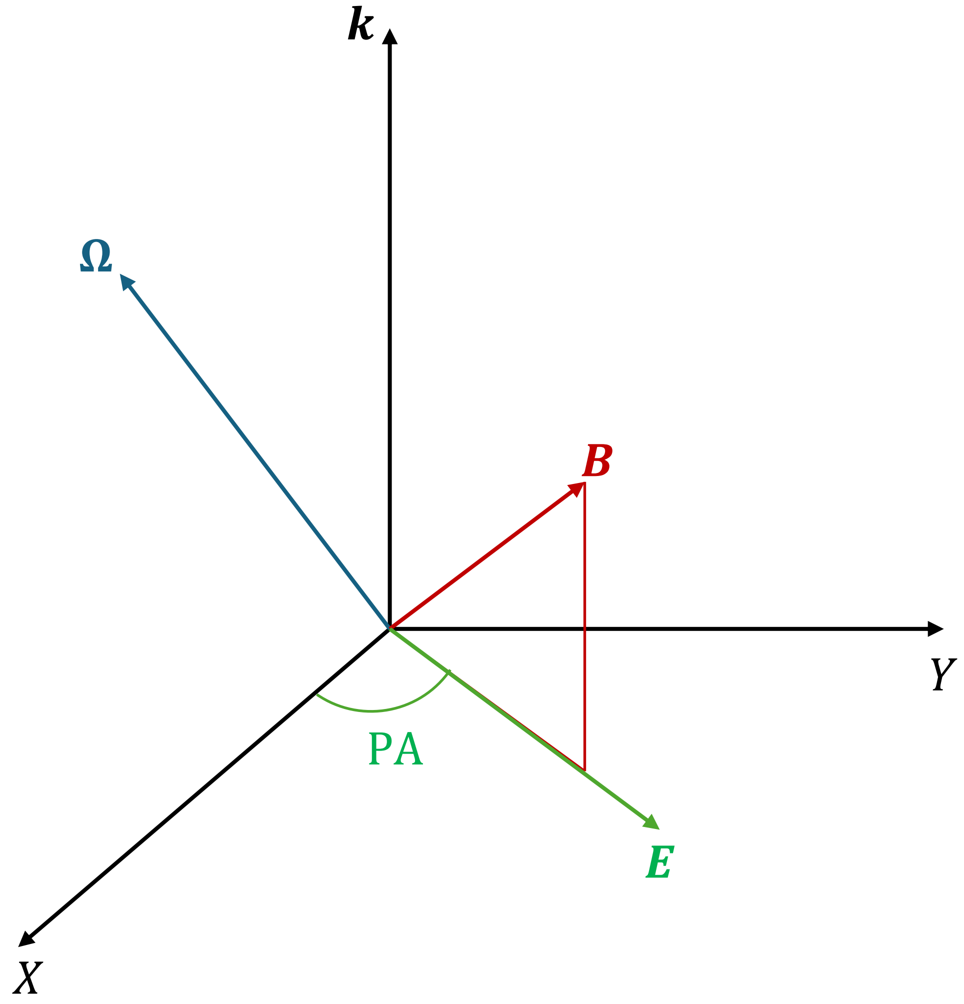

For **ordinary** photons, $\boldsymbol{E}$ is parallel to the projection of the local $\boldsymbol{B}$ field in the plane of the sky

In the (X, Y, Z) frame with $Z \parallel \ell$, if the local $\boldsymbol{B}$ has components

$$\boldsymbol{B} = \begin{pmatrix} B_X \\ B_Y \\ B_Z \end{pmatrix},$$

then the direction of $\boldsymbol{E}$ is given by

$$\boldsymbol{E} = \frac{\boldsymbol{B} - (\ell \cdot \boldsymbol{B})\ell}{|\boldsymbol{B} - (\ell \cdot \boldsymbol{B})\ell|} \quad \text{with} \quad \boldsymbol{B} - (\ell \cdot \boldsymbol{B})\ell = \begin{pmatrix} B_X \\ B_Y \\ 0 \end{pmatrix}.$$

Hence,

$$\boldsymbol{E} = \frac{1}{\sqrt{B_X^2 + B_Y^2}} \begin{pmatrix} B_X \\ B_Y \\ 0 \end{pmatrix}.$$

The position angle of $\boldsymbol{E}$ is then given by

$$\tan \mathrm{PA} = \frac{B_Y}{B_X}$$

Quantitative calculations

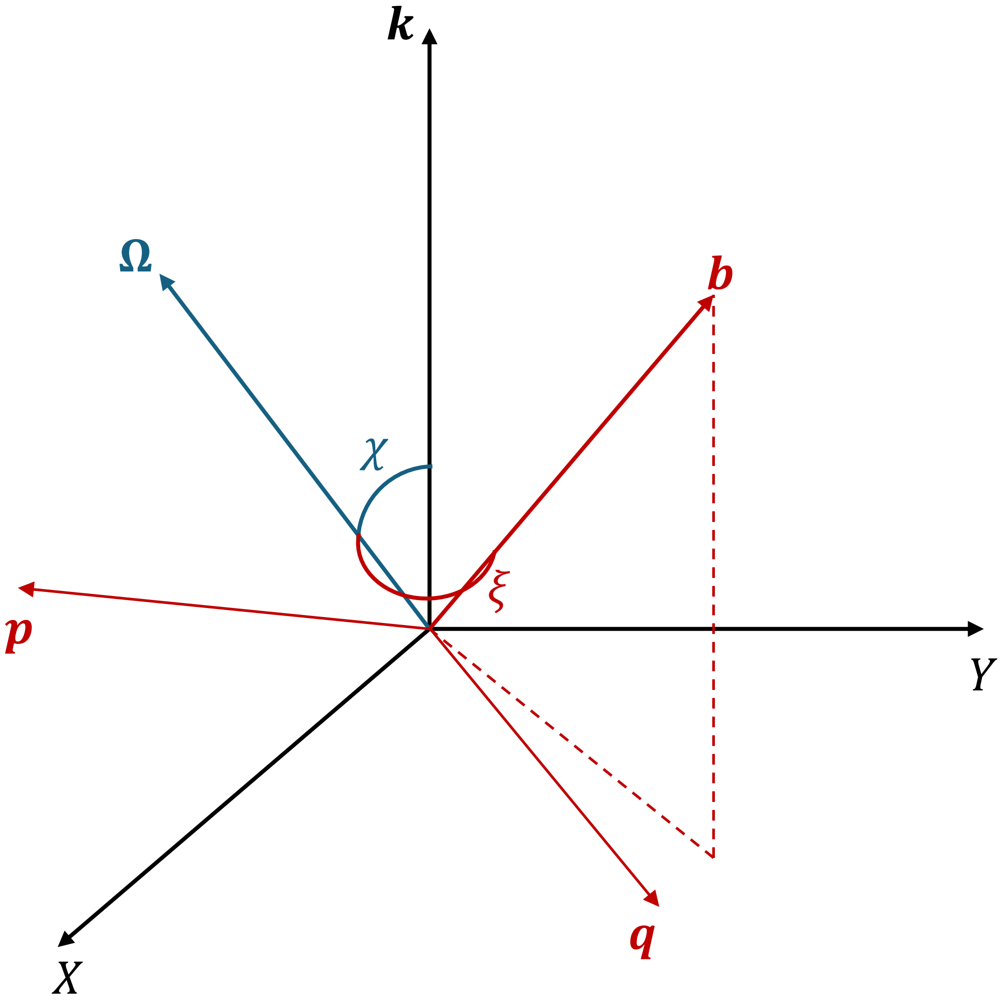

For a dipolar field, the components of $\boldsymbol{B}$ in the reference frame pqb, with $\boldsymbol{b}$ the magnetic-dipole axis are (in polar coordinates)

$$\boldsymbol{B} = \begin{pmatrix} B_r \\ B_\theta \\ B_\phi \end{pmatrix} = 2B_p \frac{R_{\mathrm{NS}}}{r^3} \begin{pmatrix} \cos\theta \\ \sin\theta/2 \\ 0 \end{pmatrix} .$$

Quantitative calculations

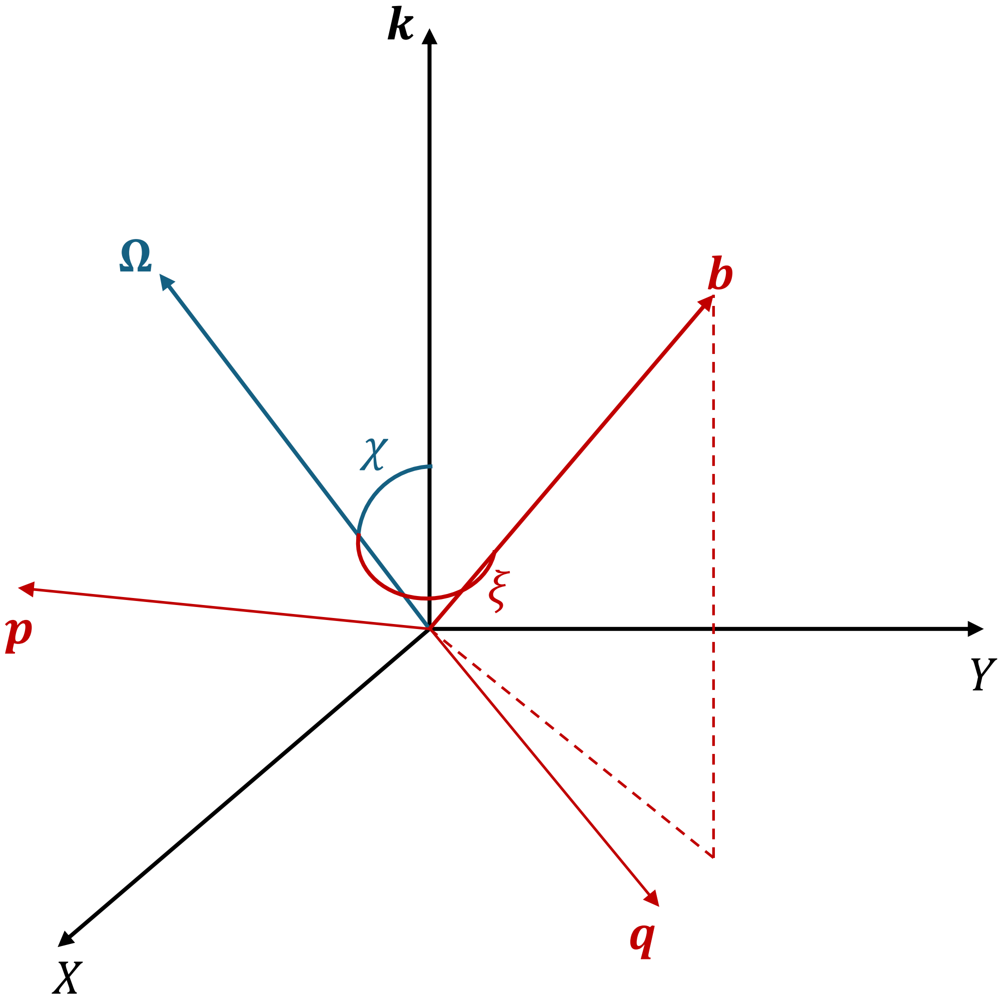

The components B_X and B_Y in the LOS frame (necessary to obtain PA) are given as

$$B_X = B_p p_X + B_q q_X + B_b b_X$$
$$B_Y = B_p P_Y + B_q q_Y + B_b b_Y$$

with

$$\boldsymbol{p} = \begin{pmatrix} p_X \\ p_Y \\ P_Z \end{pmatrix} = \begin{pmatrix} -\sin\chi\sin\xi - \cos\chi\cos\xi\cos\gamma \\ \cos\xi\sin\gamma \\ \sin\chi\cos\xi\cos\gamma - \cos\chi\sin\xi \end{pmatrix}$$

$$\boldsymbol{q} = \begin{pmatrix} -\cos\chi\sin\gamma \\ -\cos\gamma \\ \sin\chi\sin\gamma \end{pmatrix} \qquad \boldsymbol{b} = \begin{pmatrix} \sin\chi\cos\xi - \cos\chi\sin\xi\cos\gamma \\ \sin\xi\sin\gamma \\ \cos\chi\cos\xi + \sin\chi\sin\xi\cos\gamma \end{pmatrix}$$

and

$$B_p = \sin\theta\cos\phi\, B_r + \cos\theta\cos\phi\, B_\theta - \sin\phi\, B_\phi$$
$$B_q = \sin\theta\sin\phi\, B_r + \cos\theta\sin\phi\, B_\theta + \cos\phi\, B_\phi$$
$$B_b = \cos\theta\, B_r - \sin\theta B_\theta$$

Quantitative calculations

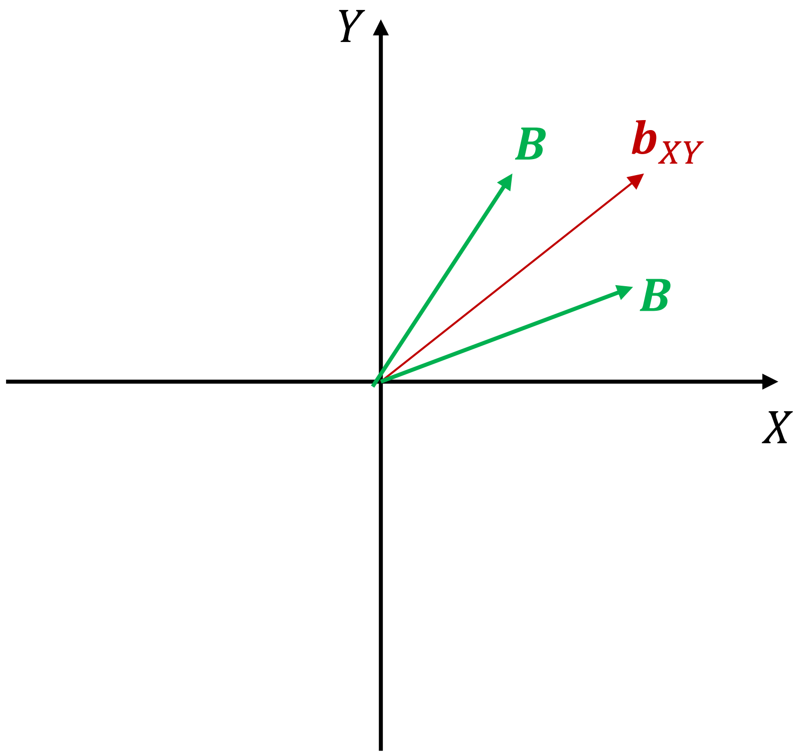

The (vectorial) sum of the $\boldsymbol{E}$-vector ($\boldsymbol{B}$-vector for ordinary photons) projections translates into the integrals

$$B_X \rightarrow \int B_X d\Omega \qquad B_Y \rightarrow \int B_Y \, d\Omega$$

over the part in view of the emitting region. $d\Omega$ can be written as the element $\sin\theta \, d\theta d\phi$ in the pqb frame, provided that the integration domain is extended over the θ and ϕ intervals which are indeed in view (at each γ).

Since $p_{X,Y}$, $q_{X,Y}$ and $b_{X,Y}$ only depend on χ, ξ and γ (not on θ and ϕ), the problem reduces to three integrals for each component,

$$\int B_X d\Omega = p_X \int B_p \, d\Omega + q_X \int B_q \, d\Omega + b_X \int B_b \, d\Omega$$

$$\int B_Y d\Omega = p_Y \int B_p \, d\Omega + q_Y \int B_q \, d\Omega + b_Y \int B_b \, d\Omega$$

Quantitative calculations

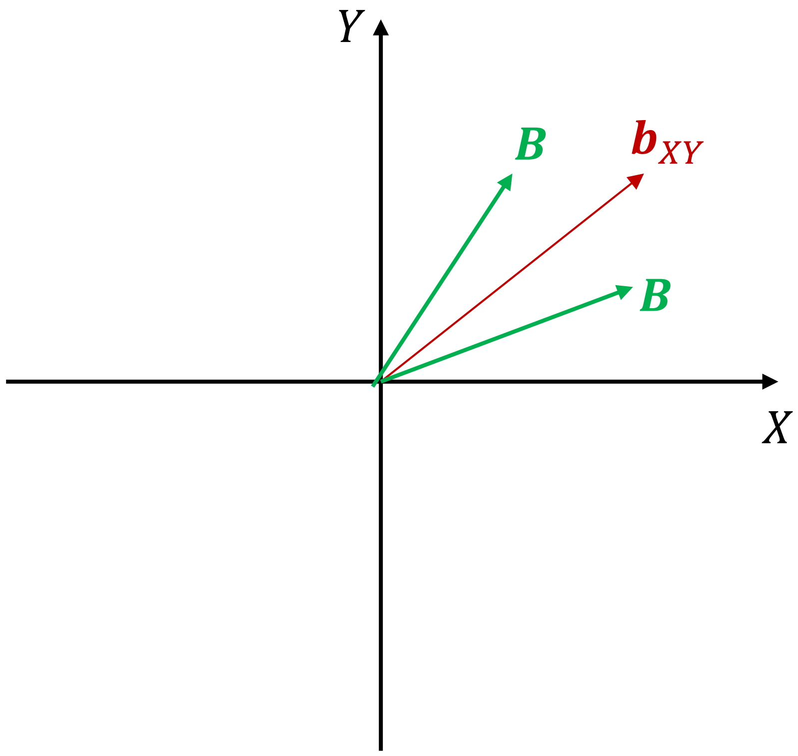

Considering the integrals separately,

$$\int B_p\, d\Omega \sim \int \left(\sin\theta\cos\phi \cdot \cos\theta + \cos\theta\cos\phi \cdot \frac{\sin\theta}{2} \right) \cdot \sin\theta\, d\theta d\phi$$
$$= \int \sin^2\theta\cos\theta\cos\phi\, d\theta d\phi + \frac{1}{2}\int \sin^2\theta\cos\theta\cos\phi\, d\theta d\phi$$
$$= \frac{3}{2}\int \sin^2\theta\cos\theta\cos\phi\, d\theta d\phi \equiv \mathcal{I}_p$$

$$\int B_q\, d\Omega \sim \int \left(\sin\theta\sin\phi \cdot \cos\theta + \cos\theta\sin\phi \cdot \frac{\sin\theta}{2} \right) \cdot \sin\theta\, d\theta d\phi$$
$$= \int \sin^2\theta\cos\theta\sin\phi\, d\theta d\phi + \frac{1}{2}\int \sin^2\theta\cos\theta\sin\phi\, d\theta d\phi$$
$$= \frac{3}{2}\int \sin^2\theta\cos\theta\sin\phi\, d\theta d\phi \equiv \mathcal{I}_q$$

$$\int B_b d\Omega \sim \int \left(\cos\theta \cdot \cos\theta - \sin\theta \cdot \frac{\sin\theta}{2} \right) \cdot \sin\theta\, d\theta d\phi$$
$$= \int \cos^2\theta\sin\theta\, d\theta d\phi - \frac{1}{2}\int \sin^3\theta\, d\theta d\phi \equiv \mathcal{I}_b$$

Quantitative calculations

All the integral should be extended over an integration domain depending on both the extension of the emission region and the field of view. In particular,

$$\cos\theta = \frac{R_{\rm NS}\sin\Theta}{r_{\rm pl}}(\cos\Phi\sin\chi\cos\xi + \sin\Phi\sin\xi\sin\gamma - \cos\Phi\cos\chi\sin\xi\cos\gamma) + \sqrt{1-\left(\frac{R_{\rm NS}}{r_{\rm pl}}\sin\Theta\right)^2}\,(\cos\chi\cos\xi + \sin\chi\sin\xi\cos\gamma)$$

$$\cos\phi = \frac{R_{\rm NS}\sin\Theta}{r_{\rm pl}\sin\theta}(\sin\Phi\cos\xi\sin\gamma - \cos\Phi\sin\chi\sin\xi - \cos\Phi\cos\chi\cos\xi\cos\gamma) + \sqrt{\frac{r_{\rm pl}^2-(R_{\rm NS}\sin\Theta)^2}{r_{\rm pl}^2\sin^2\theta}}\,(\sin\chi\cos\xi\cos\gamma - \cos\chi\sin\xi)$$

with Θ and Φ colatitude and azimuth wrt the LOS, respectively.

Quantitative calculations

Peculiar cases

Given that $\mathcal{I}_q$ contains the integral of $\sin\phi$, it gives 0 if the emitting region has symmetry in ϕ around the magnetic pole (i.e. if for each point at ϕ there is a point at $2\pi - \phi$**, azimuthal symmetry wrt $\boldsymbol{b}$**)

Given that both $\mathcal{I}_p$ and $\mathcal{I}_q$ contain the integral of $\sin^2\theta \cos\theta \, d\theta$, they give 0 if the emitting region has symmetry in θ around the magnetic equator (i.e. if for each point at θ there is a point at $\pi - \theta$, **colatitudinal symmetry wrt $\boldsymbol{b}$**)

In all the other case (for example a single polar cap), the integrals $\mathcal{I}_p$ and $\mathcal{I}_q$ give 0 only if all the magnetic azimuths ϕ at a given θ are in view at the same rotational phase (integral in ϕ from 0 to 2π, **symmetry with respect to the field of view**)

The integral $\mathcal{I}_b$ does not give zero in the same conditions, since it does not depend on ϕ and depends on θ only through $\cos^2\theta$ (or $\sin^2\theta$) – It gives 0 only in degenerate cases (e.g. $\xi = 0$, where the RVM oscillation vanishes)

Quantitative calculations

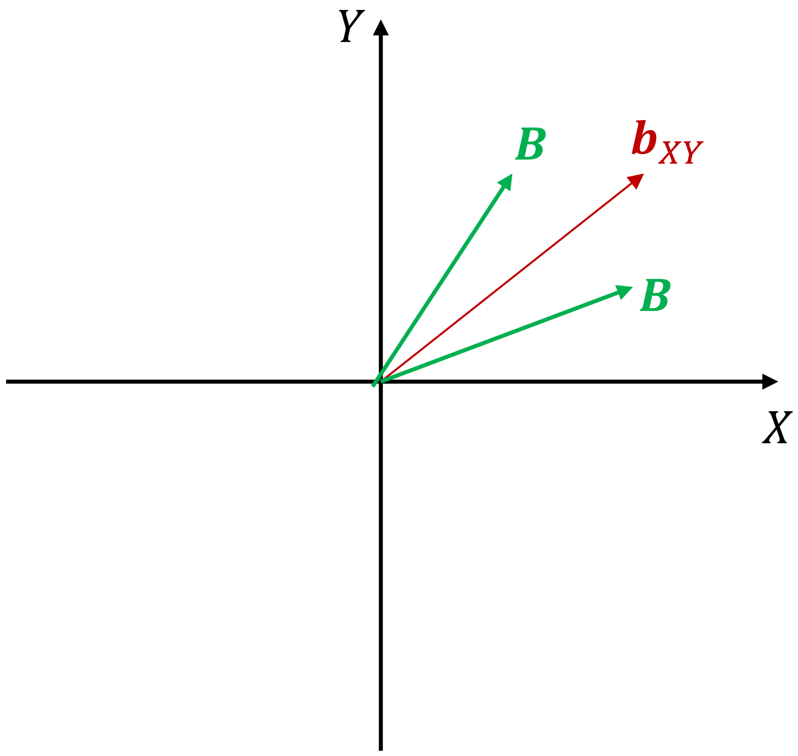

Hence, under the required symmetries around $\boldsymbol{b}$ and ℓ, it results

$$\tan \mathrm{PA} = \frac{\int B_Y d\Omega}{\int B_X d\Omega} = \frac{b_Y \mathcal{I}_b}{b_X \mathcal{I}_b} = \frac{b_Y}{b_X} = \frac{\sin\xi \sin\gamma}{\cos\chi\cos\xi + \sin\chi\sin\xi\cos\gamma}$$

which is the RVM